

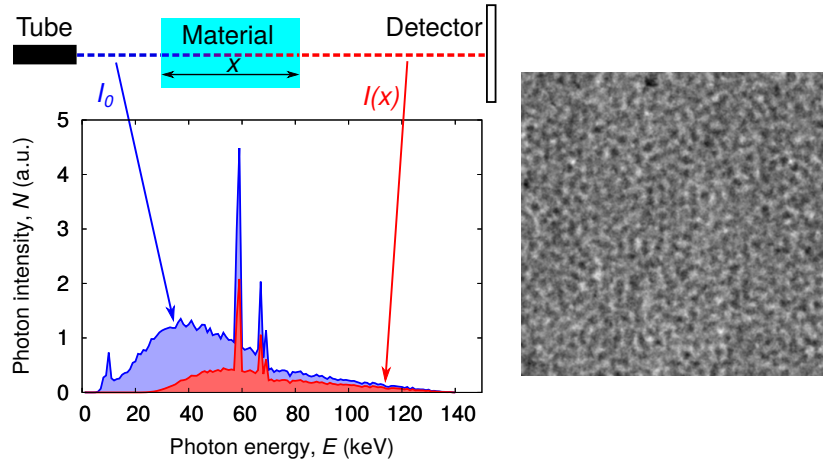


PhD defense
Manuel Baur

Funded by the German
Federal Ministry for
Economic Affairs and
Energy, grant no. 50WM

1653

X-ray radiography of granular systems – particle densities and dynamics



X-ray radiography of granular systems – particle densities and dynamics

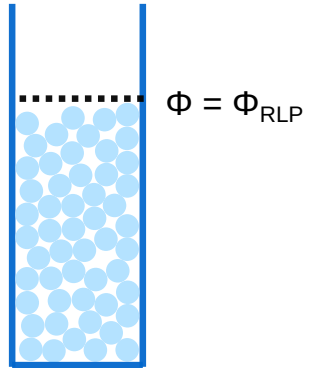


X-ray radiography of granular systems – particle densities and dynamics

Volume fraction



$$\Phi = \frac{V_{\text{Particles}}}{V_{\text{Container}}}$$

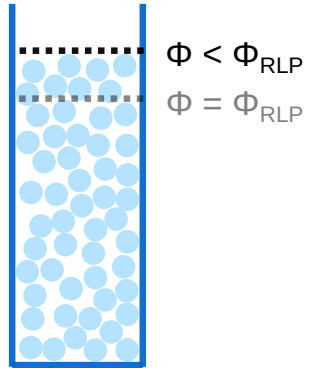


X-ray radiography of granular systems – particle densities and dynamics

Volume fraction



$$\Phi = \frac{V_{\text{Particles}}}{V_{\text{Container}}}$$

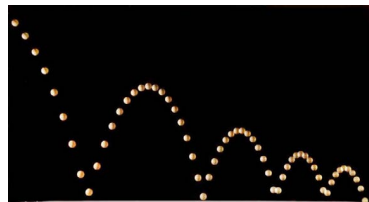


X-ray radiography of granular systems – particle densities and dynamics

Volume fraction

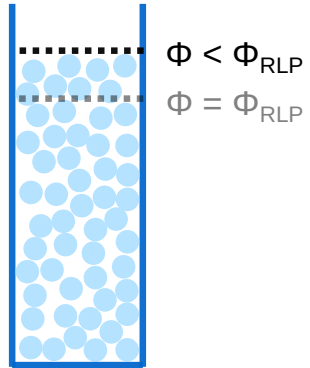


Dissipative interactions



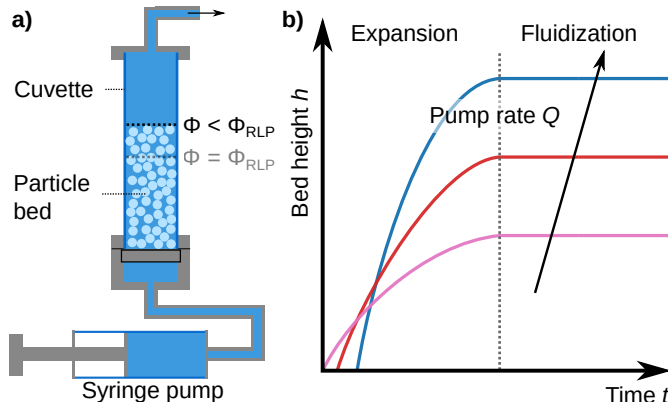
Driscoll *et al* (2016)

$$\Phi = \frac{V_{\text{Particles}}}{V_{\text{Container}}}$$



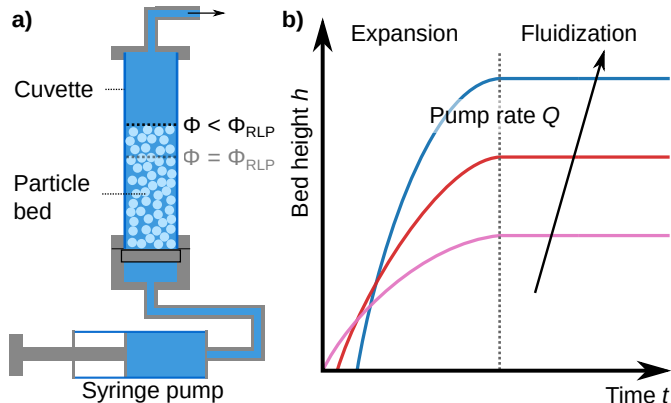
X-ray radiography of granular systems – particle densities and dynamics

Fluidized bed



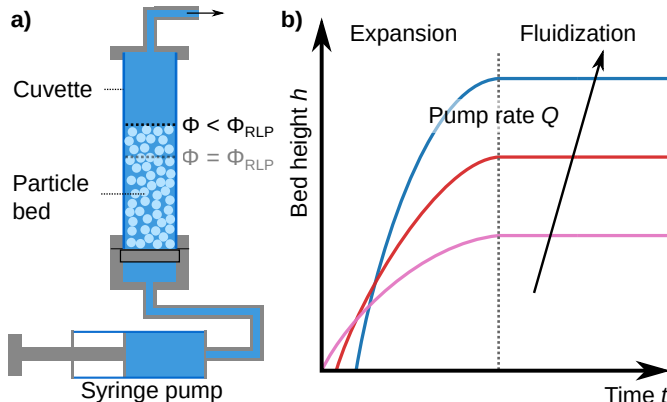
X-ray radiography of granular systems – particle densities and dynamics

Fluidized bed



X-ray radiography of granular systems – particle densities and dynamics

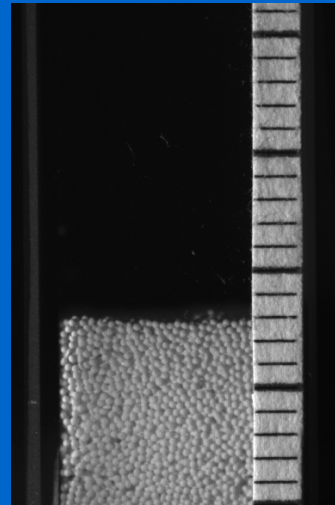
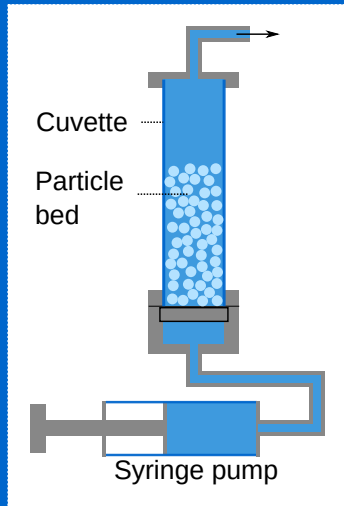
Fluidized bed



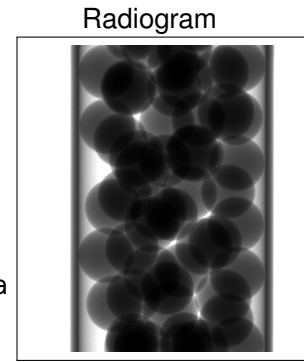
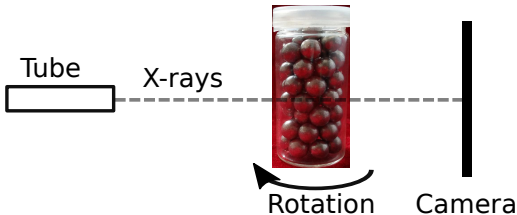
Fluidized bed reactor

"Lack of understanding:
It is very difficult to predict and calculate the **complex mass** [...] **flows** within the bed."

Particulate flows are **opaque**

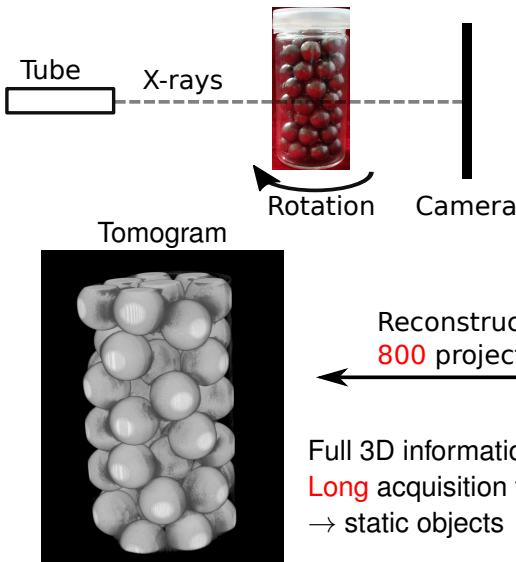


X-ray radiography



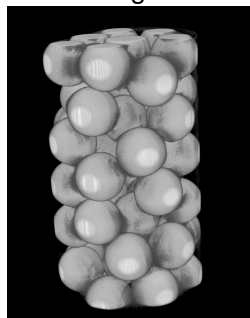
2D projections of 3D object
Short acquisition time

X-ray radiography



Radiogram

2D projections of 3D object
Short acquisition time

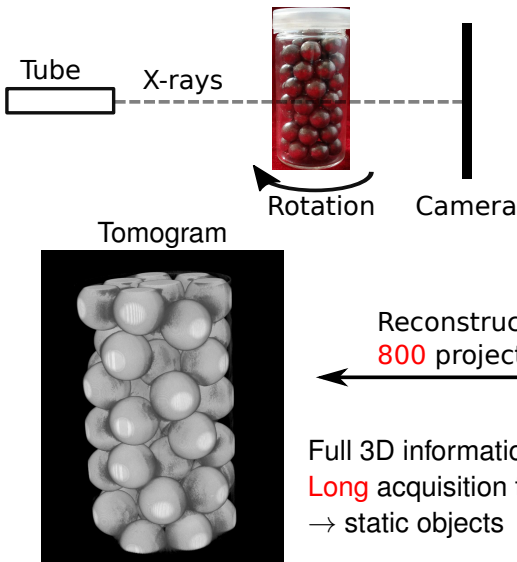


Tomogram

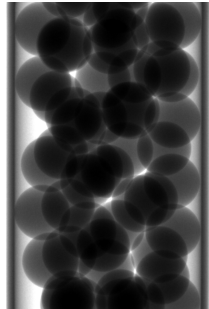
Reconstruction from
800 projections

Full 3D information
Long acquisition time
→ static objects

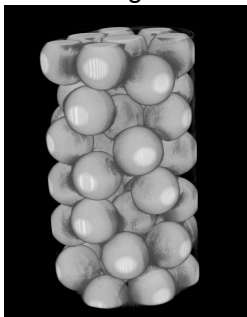
X-ray radiography



Radiogram



2D projections of 3D object
Short acquisition time

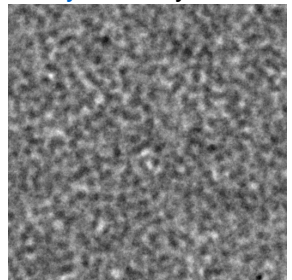


Tomogram

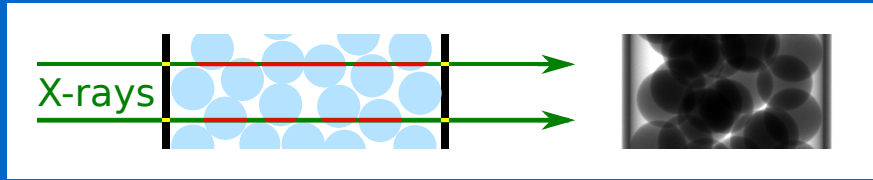
Reconstruction from
800 projections

Full 3D information
Long acquisition time
→ static objects

Dynamic system



Measuring the volume fraction of **dynamic** granular systems

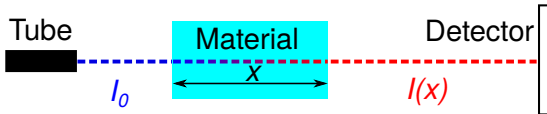


Correction of beam hardening
in X-ray radiograms

Baur *et al*, *Rev. Sci. Instrum.* (2019)

In collaboration with Norman Uhlmann, Fraunhofer EZRT

Attenuation of X-rays

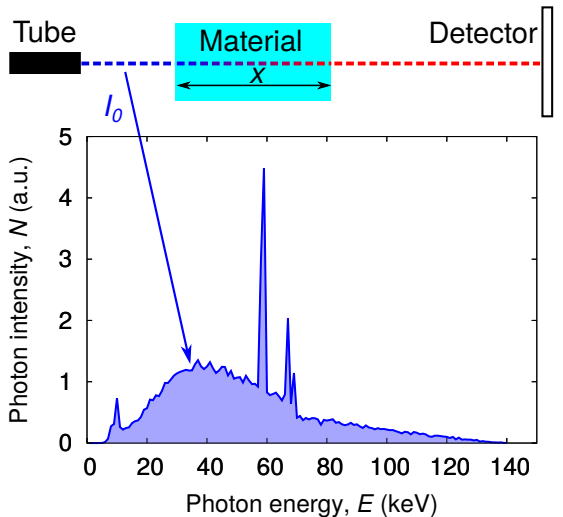


Beer-Lambert's law

$$I(x) = I_0 \exp(-\mu x)$$

$$\text{Thickness: } x = -\frac{1}{\mu} \ln \frac{I(x)}{I_0}$$

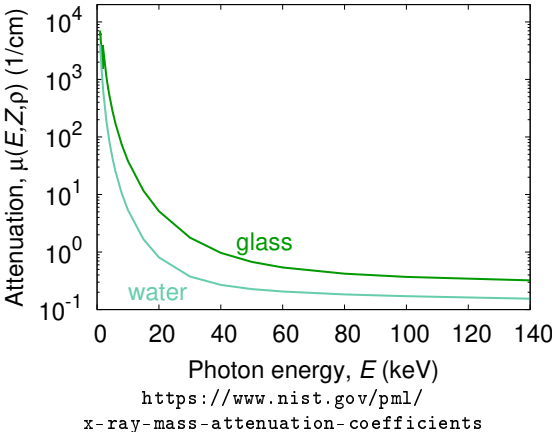
Attenuation of X-rays



Beer-Lambert's law

$$\mu \neq \text{const}$$
$$I(x) = I_0 \exp(-\mu(E, Z, \rho)x)$$

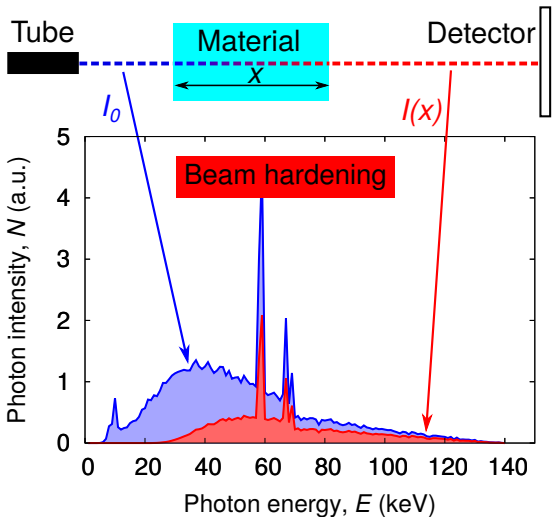
Thickness: $x = ?$



<https://www.nist.gov/pml/>

x-ray-mass-attenuation-coefficients

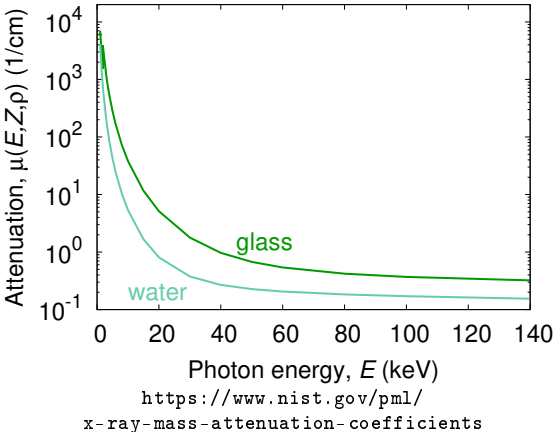
Attenuation of X-rays



Beer-Lambert's law

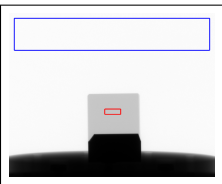
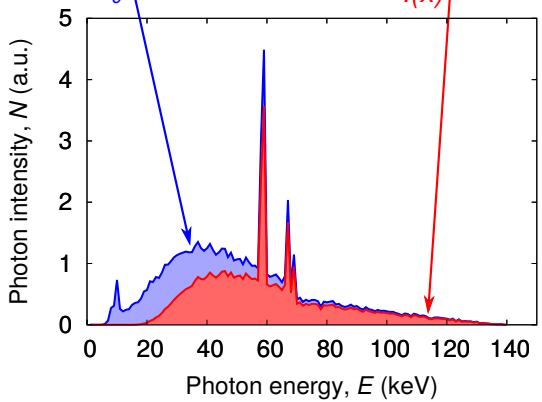
$$\mu \neq \text{const}$$
$$I(x) = I_0 \exp(-\mu(E, Z, \rho)x)$$

Thickness: $x = ?$



[https://www.nist.gov/pml/
x-ray-mass-attenuation-coefficients](https://www.nist.gov/pml/x-ray-mass-attenuation-coefficients)

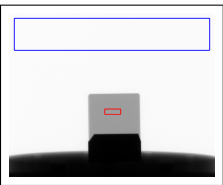
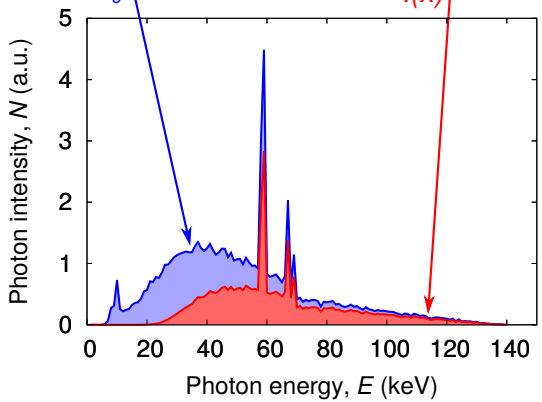
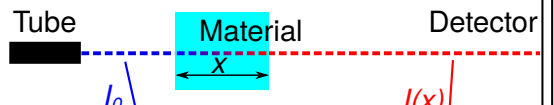
The effective attenuation, $\mu_{\text{eff}}(x)$



effective attenuation:

$$I(x) = I_0 \exp(-\mu_{\text{eff}}(x) x)$$

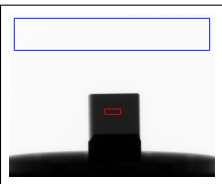
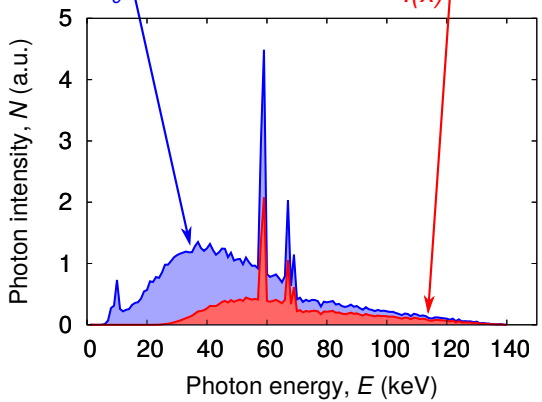
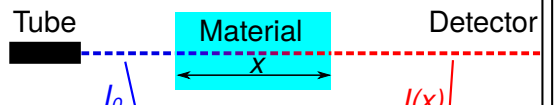
The effective attenuation, $\mu_{\text{eff}}(x)$



effective attenuation:

$$I(x) = I_0 \exp(-\mu_{\text{eff}}(x) x)$$

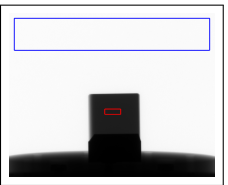
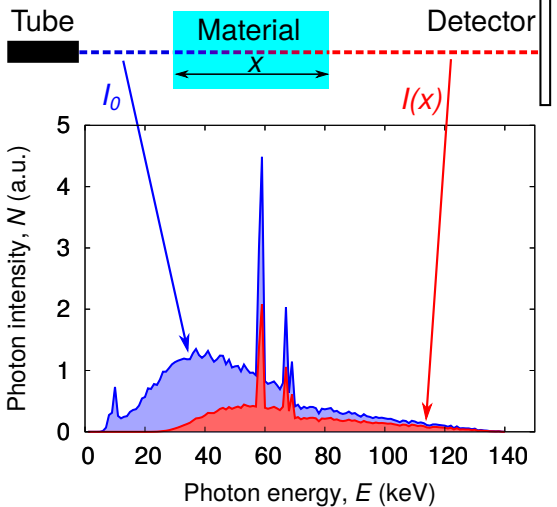
The effective attenuation, $\mu_{\text{eff}}(x)$



effective attenuation:

$$I(x) = I_0 \exp(-\mu_{\text{eff}}(x) x)$$

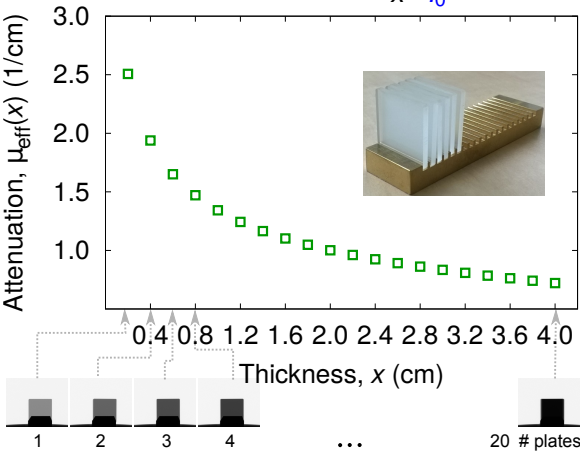
The effective attenuation, $\mu_{\text{eff}}(x)$



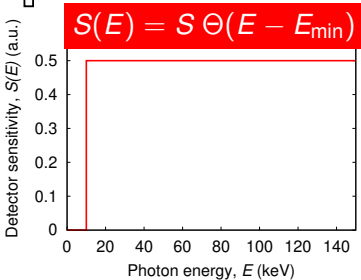
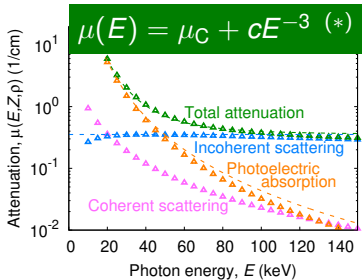
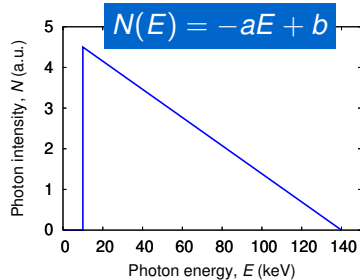
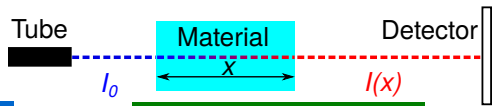
effective attenuation:

$$I(x) = I_0 \exp(-\mu_{\text{eff}}(x) x)$$

$$\mu_{\text{eff}}(x) = -\frac{1}{x} \frac{I(x)}{I_0}$$



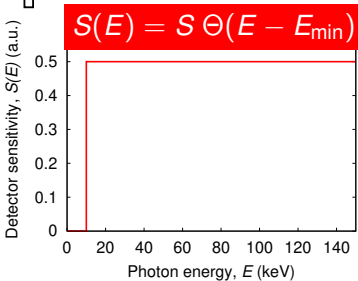
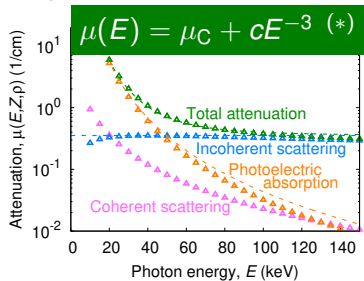
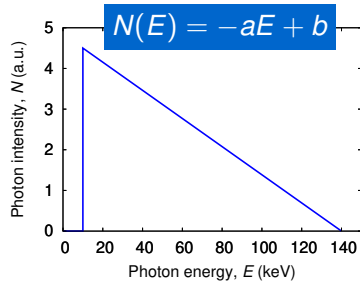
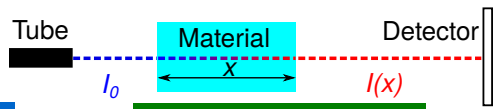
Modeling of $\mu_{\text{eff}}(x)$



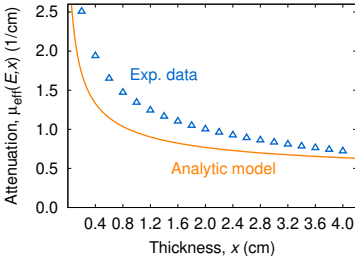
$$I(x) \propto \int N(E) \exp\{-\mu(E, Z, \rho)x\} S(E) dE$$

(*) XCOM supplied by NIST

Modeling of $\mu_{\text{eff}}(x)$

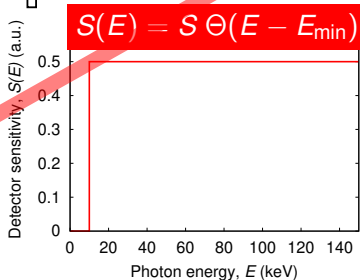
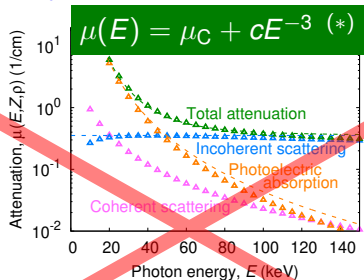
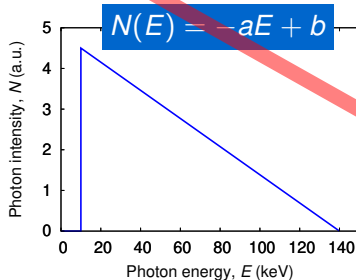
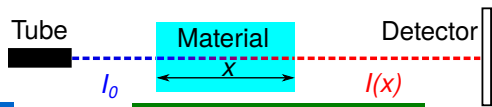


$$\begin{aligned} I(x) &\propto \int N(E) \exp\{-\mu(E, Z, \rho)x\} S(E) dE \\ &\propto S \int_{E_{\min}}^{E_{\max}} (-aE + b) \exp\{-(\mu_C + cE^{-3})x\} dE \end{aligned}$$



(*) XCOM supplied by NIST

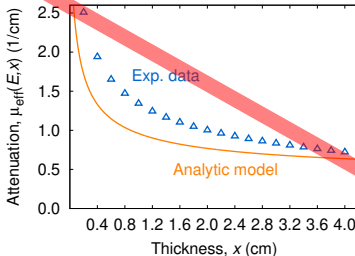
Modeling of $\mu_{\text{eff}}(x)$



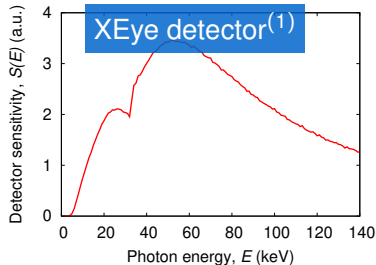
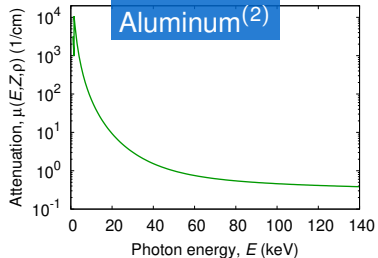
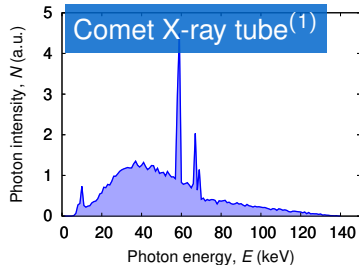
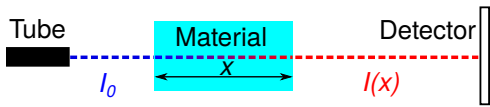
$$I(x) \propto \int N(E) \exp\{-\mu(E, Z, \rho)x\} S(E) dE$$

$$\propto S \int_{E_{\min}}^{E_{\max}} (-aE + b) \exp\{-(\mu_C + cE^{-3})x\} dE$$

(*) XCOM supplied by NIST



Numerical approx. of $\mu_{\text{eff}}(x)$



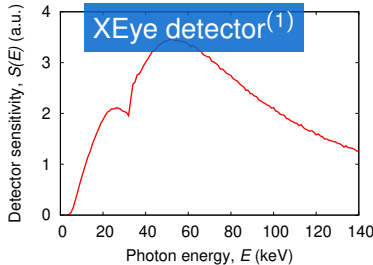
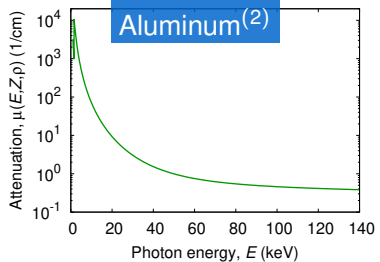
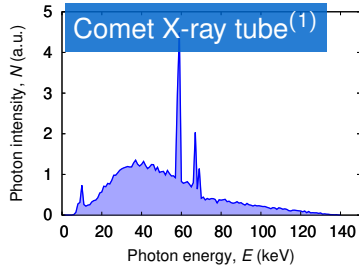
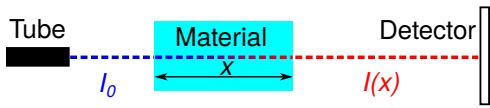
$$I(x) \propto \int N(E) \exp\{-\mu(E, Z, \rho)x\} S(E) dE$$

$$\int \rightarrow \sum$$

(1) Supplied by Norman Uhlmann, Fraunhofer EZRT

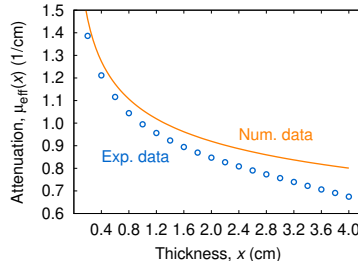
(2) XCOM supplied by NIST

Numerical approx. of $\mu_{\text{eff}}(x)$



$$I(x) \propto \int N(E) \exp\{-\mu(E, Z, \rho)x\} S(E) dE$$

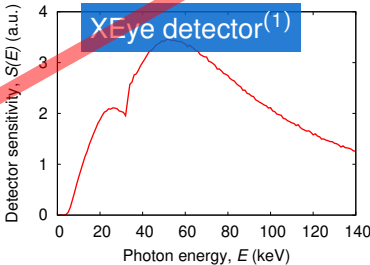
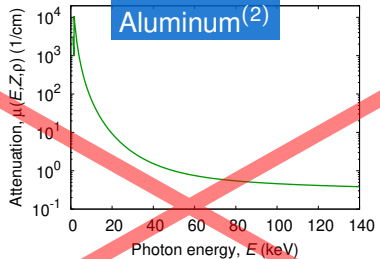
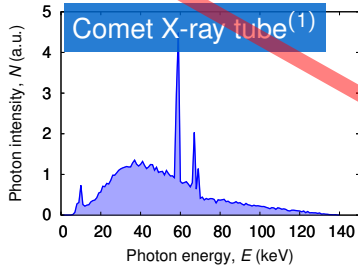
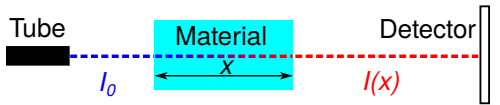
$$\int \rightarrow \sum$$



(1) Supplied by Norman Uhlmann, Fraunhofer EZRT

(2) XCOM supplied by NIST

Numerical approx. of $\mu_{\text{eff}}(x)$

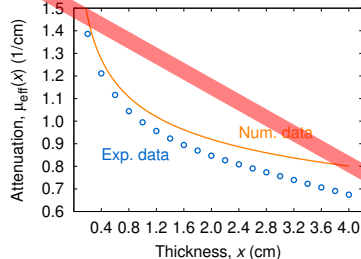


$$I(x) \propto \int N(E) \exp\{-\mu(E, Z, \rho)x\} S(E) dE$$

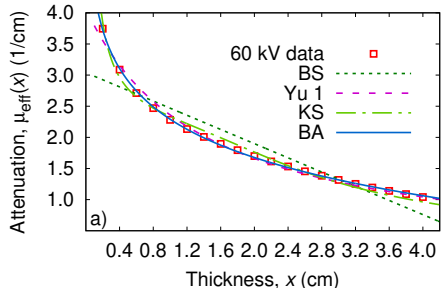
$$\int \rightarrow \sum$$

(1) Supplied by Norman Uhlmann, Fraunhofer EZRT

(2) XCOM supplied by NIST



Heuristic model functions for $\mu_{\text{eff}}(x)$



$$\mu_{\text{eff}}(x) = \mu_0 - \lambda x$$

Bjärngard & Shackford
(1994)

$$\mu_{\text{eff}}(x) = \frac{\mu_0}{1 + \lambda x}$$

Yu *et al.* (1997)

$$\mu_{\text{eff}}(x) = \mu(E_{\text{max}}) + \frac{2\mu_1}{x\sqrt{-\lambda_1^2 + 4\lambda_2}} \times$$

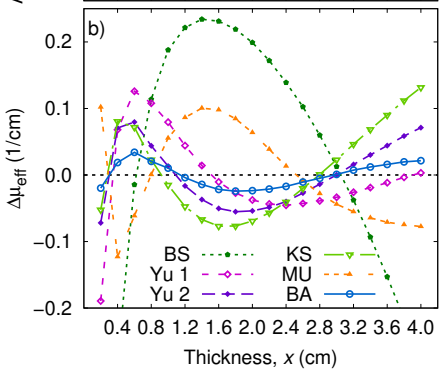
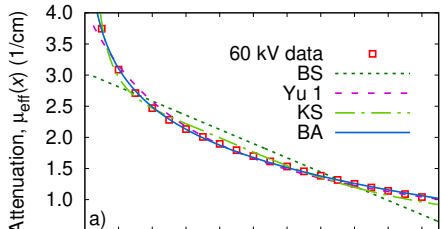
$$\left[\arctan\left(\frac{\lambda_1 + 2\lambda_2 x}{\sqrt{-\lambda_1^2 + 4\lambda_2}}\right) - \arctan\left(\frac{\lambda_1}{\sqrt{-\lambda_1^2 + 4\lambda_2}}\right) \right]$$

Kleinschmidt (1999)

$$\mu_{\text{eff}}(x) = a + \frac{b}{x^\alpha}$$

Baur *et al.* (2019)
(this work)

Heuristic model functions for $\mu_{\text{eff}}(x)$



$$\mu_{\text{eff}}(x) = \mu_0 - \lambda x$$

Bjärngard & Shackford
(1994)

$$\mu_{\text{eff}}(x) = \frac{\mu_0}{1 + \lambda x}$$

$$\mu_{\text{eff}}(x) = \frac{\mu_0}{(1 + \lambda x)^\beta}$$

Yu *et al.* (1997)

$$\mu_{\text{eff}}(x) = \mu(E_{\text{max}}) + \frac{2\mu_1}{x\sqrt{-\lambda_1^2 + 4\lambda_2}} \times \left[\arctan\left(\frac{\lambda_1 + 2\lambda_2 x}{\sqrt{-\lambda_1^2 + 4\lambda_2}}\right) - \arctan\left(\frac{\lambda_1}{\sqrt{-\lambda_1^2 + 4\lambda_2}}\right) \right]$$

Kleinschmidt (1999)

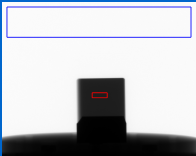
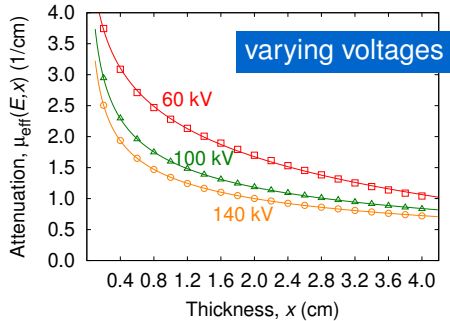
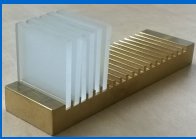
$$\mu_{\text{eff}}(x) = -\frac{1}{x} \ln [A + B \exp(-x/C)]$$

Mudde *et al.* (2008)

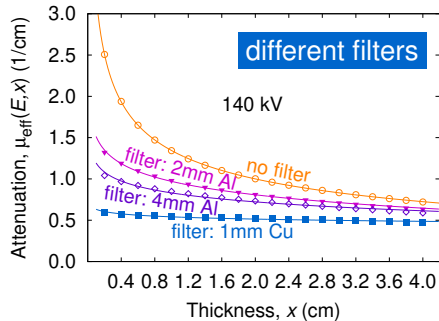
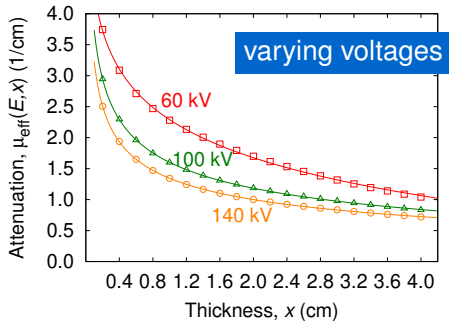
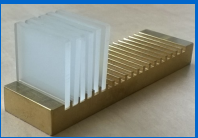
$$\mu_{\text{eff}}(x) = a + \frac{b}{x^\alpha}$$

Baur *et al.* (2019)
(this work)

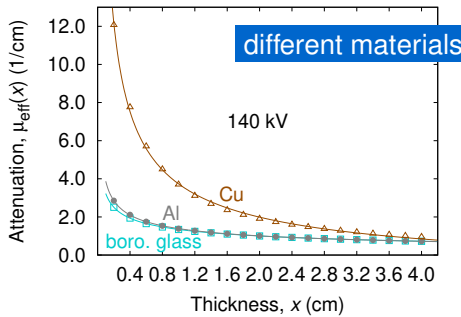
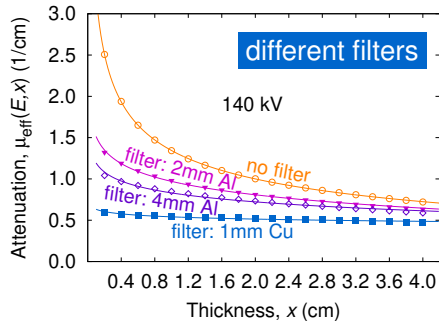
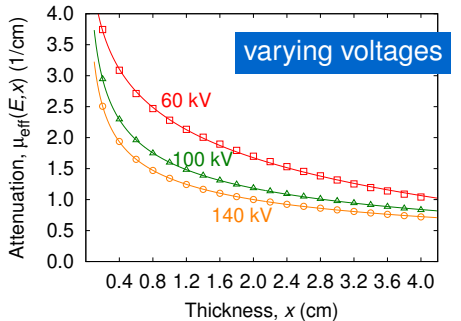
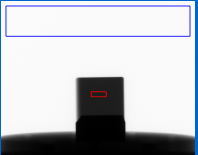
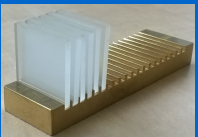
Universality of
 $\mu_{\text{eff}}(x) = a + \frac{b}{x^\alpha}$



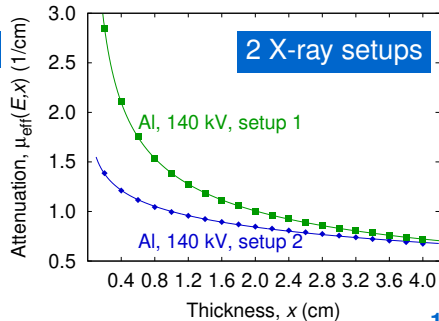
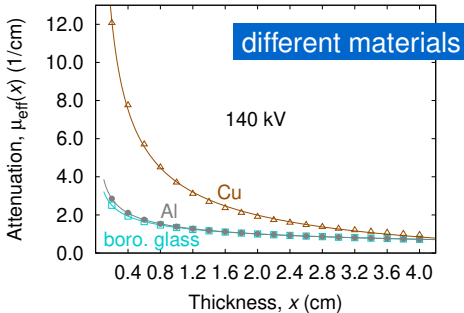
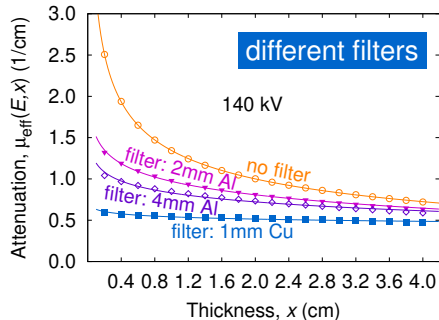
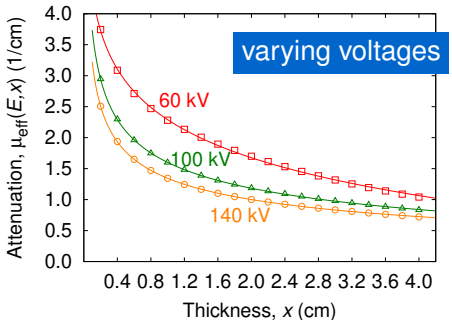
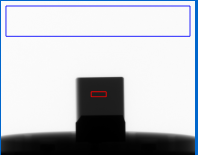
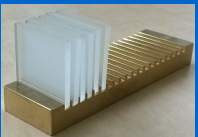
Universality of
 $\mu_{\text{eff}}(x) = a + \frac{b}{x^\alpha}$



Universality of
 $\mu_{\text{eff}}(x) = a + \frac{b}{x^\alpha}$



Universality of
 $\mu_{\text{eff}}(x) = a + \frac{b}{x^\alpha}$



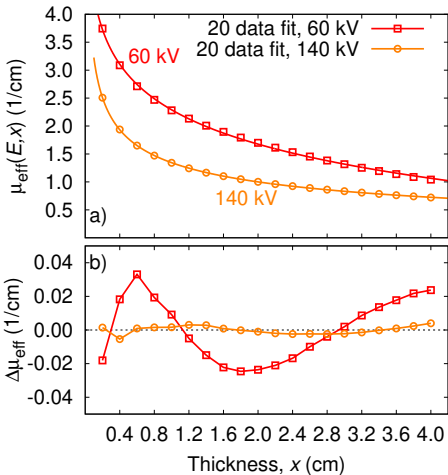
Determining the material thickness x

Generalized Beer-Lambert

$$I(x) = I_0 \exp(-\mu_{\text{eff}}(x) x)$$

Model function

$$\mu_{\text{eff}}(x) = a + \frac{b}{x^\alpha}$$



Determining the material thickness x

Generalized Beer-Lambert

$$I(x) = I_0 \exp(-\mu_{\text{eff}}(x) x)$$

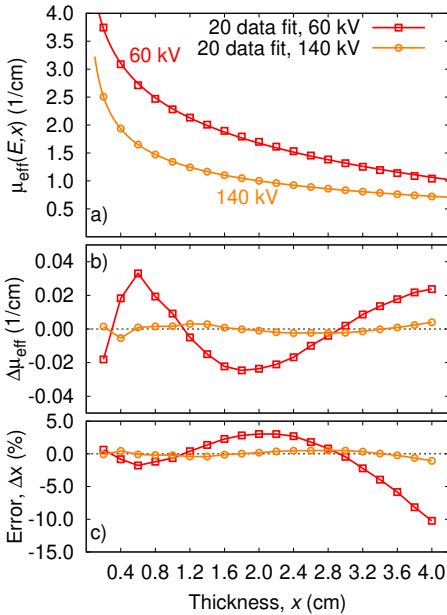
Model function

$$\mu_{\text{eff}}(x) = a + \frac{b}{x^\alpha}$$

Solve

$$ax + bx^{1-\alpha} + \ln\left(\frac{I(x)}{I_0}\right) = 0$$

e.g. Newton's method or look-up table



Determining the material thickness x

Generalized Beer-Lambert

$$I(x) = I_0 \exp(-\mu_{\text{eff}}(x) x)$$

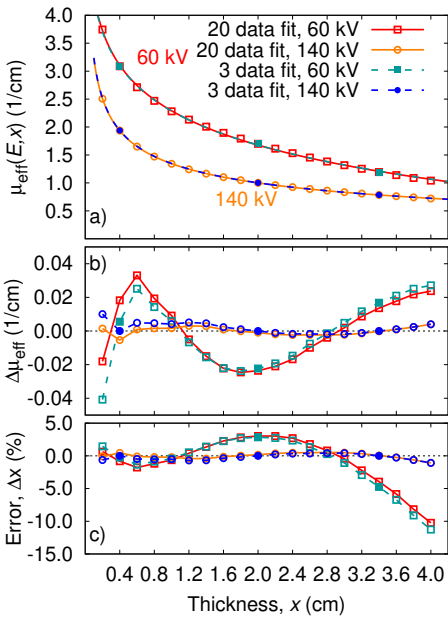
Model function

$$\mu_{\text{eff}}(x) = a + \frac{b}{x^\alpha}$$

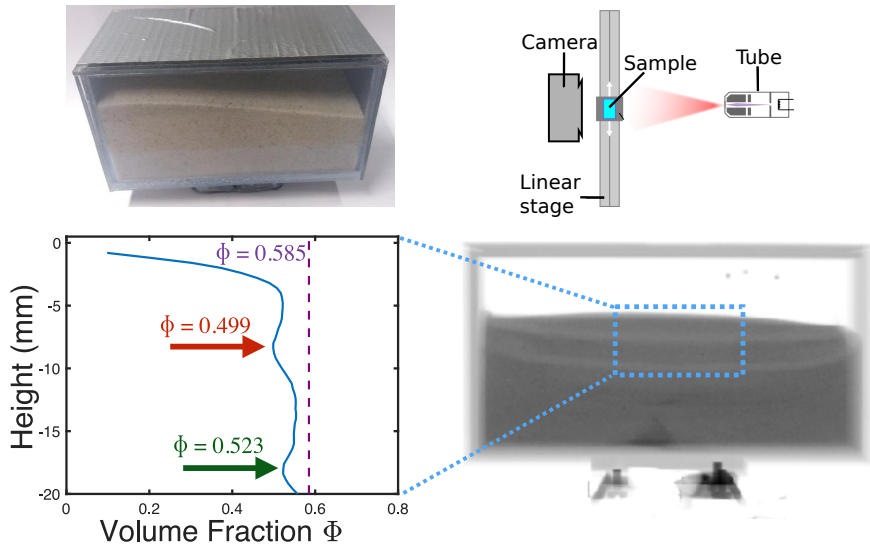
Solve

$$ax + bx^{1-\alpha} + \ln\left(\frac{I(x)}{I_0}\right) = 0$$

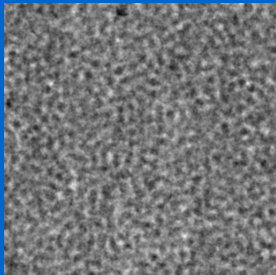
e.g. Newton's method or look-up table



Migrating shear bands in shaken granular matter, Kollmer *et al* (2020)

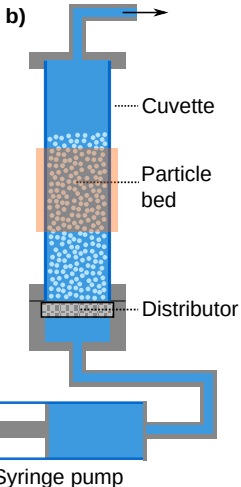
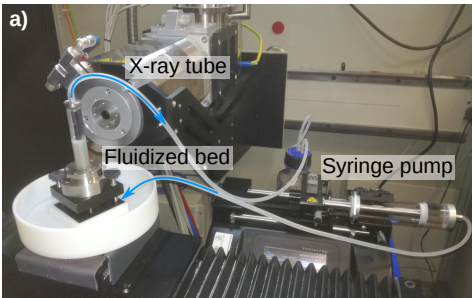


Measuring granular dynamics with X-ray Digital Fourier Analysis (X-DFA)

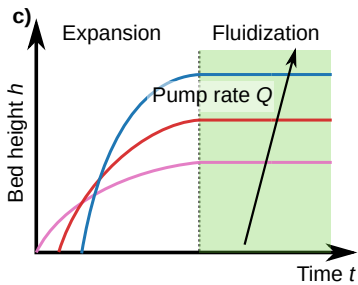
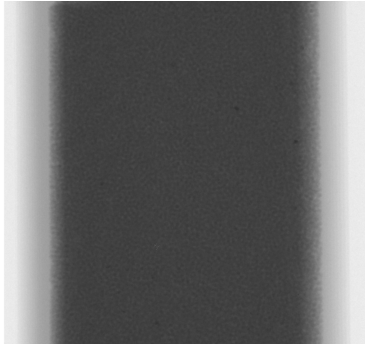


In collaboration with M. Escobedo & S. Egelhaaf, University of Düsseldorf

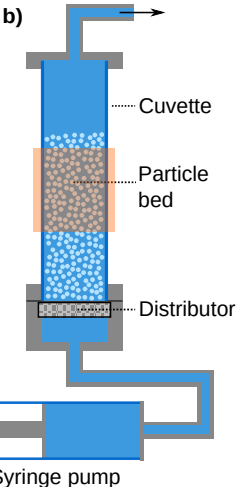
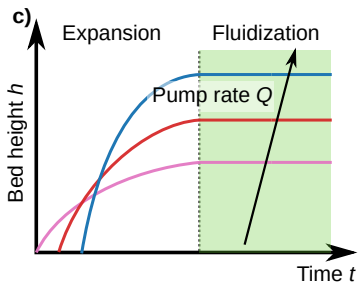
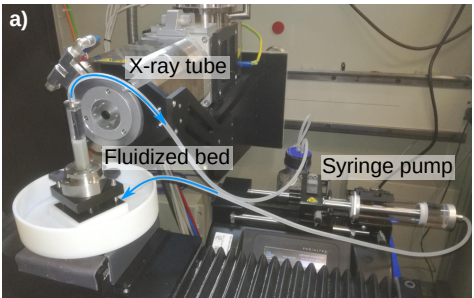
The system: A liquid fluidized bed



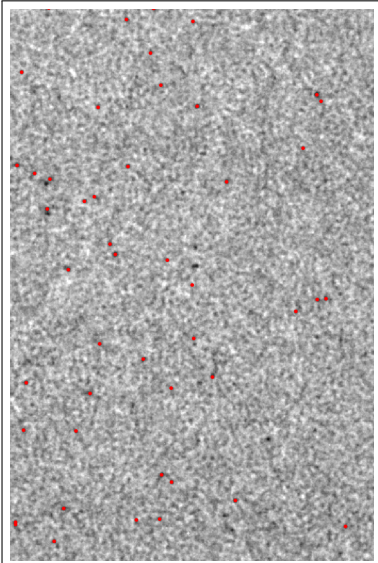
Radiogram



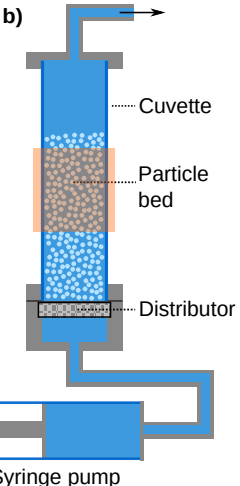
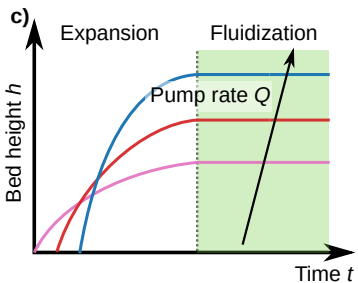
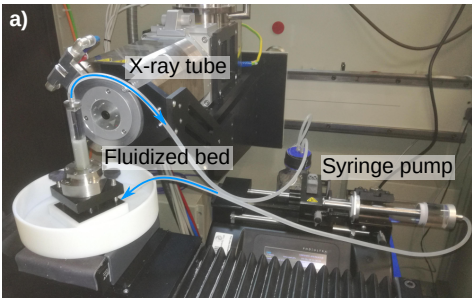
The system: A liquid fluidized bed



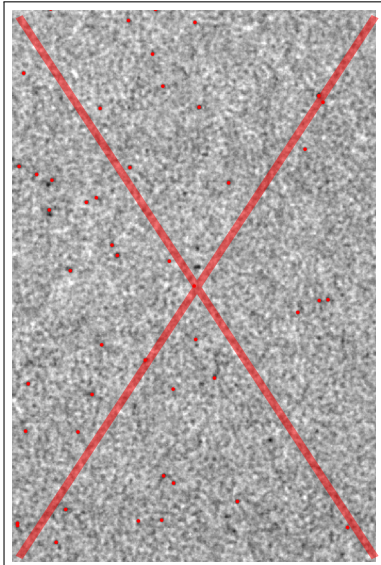
Particle tracking
Contrast: $\rho_{\text{tracer}} > \rho_{\text{bed}}$



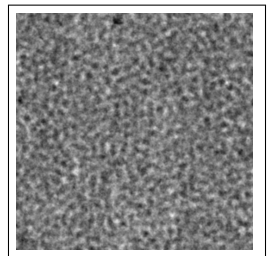
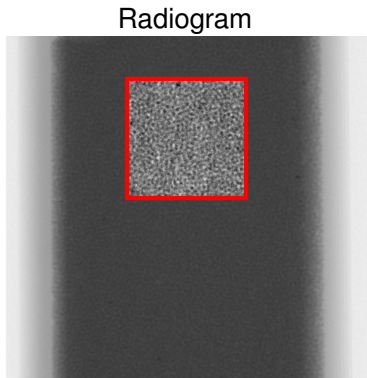
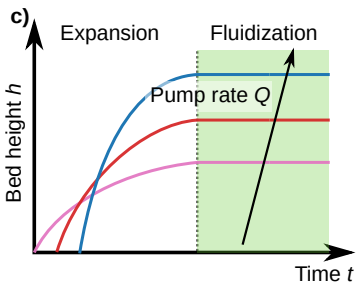
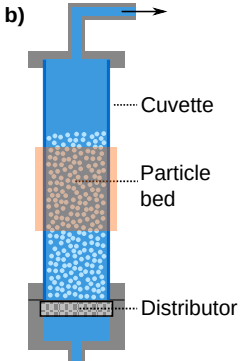
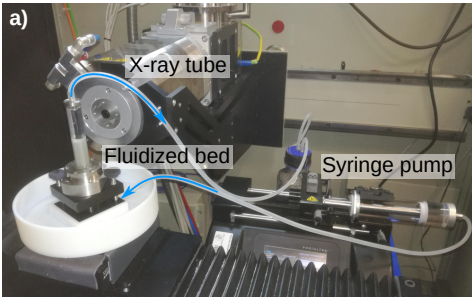
The system: A liquid fluidized bed



Particle tracking
Contrast: $\rho_{\text{tracer}} > \rho_{\text{bed}}$



The system: A liquid fluidized bed



Differential Dynamic Microscopy (DDM)

	Up to now	This work
System	Dispersion, gels	Fluidized bed
Particles	Colloids $< 1 \mu\text{m}$	Granulates ($150 - 180 \mu\text{m}$)
Volume fraction	$\Phi \leq 0.33$	$0.45 < \Phi < 0.56$
Imaging	Light microscopy	X-ray radiography
Dynamics	Brownian motion, caging, glassy, collective motion	

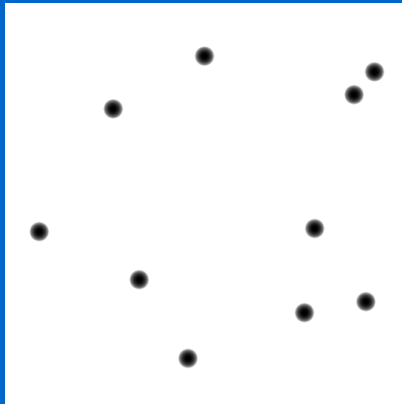
Extending Differential Dynamic Microscopy (DDM) to X-ray imaging

	Up to now	This work
System	Dispersion, gels	Fluidized bed
Particles	Colloids $< 1 \mu\text{m}$	Granulates (150 – 180) μm
Volume fraction	$\Phi \leq 0.33$	$0.45 < \Phi < 0.56$
Imaging	Light microscopy	X-ray radiography
Dynamics	Brownian motion, caging, glassy, collective motion	

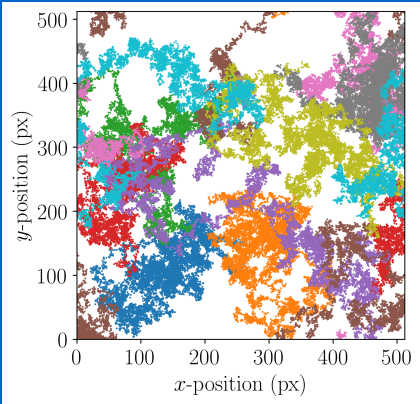
Digital Fourier Analysis of X-Ray radiograms (X-DFA)

Introduction to X-ray Digital Fourier Analysis (X-DFA)

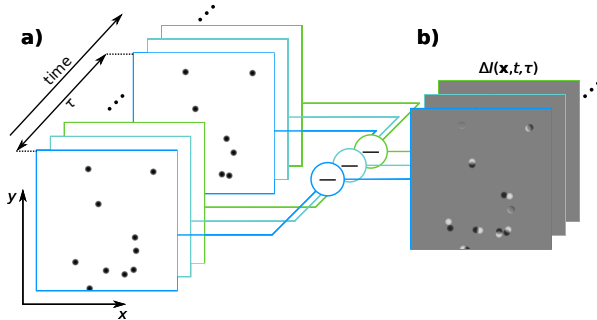
Synthetic radiograms



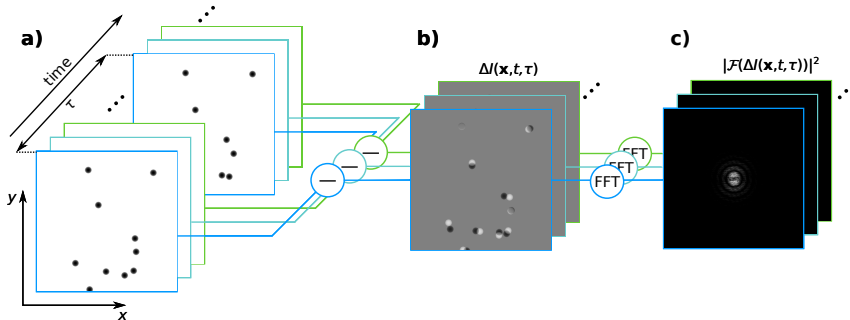
Particle trajectory



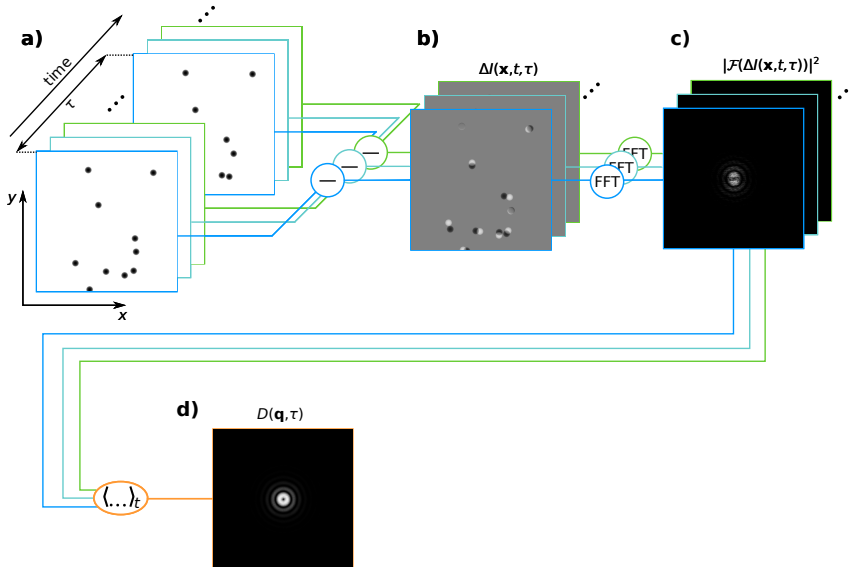
The image structure function $D(\mathbf{q}, \tau)$



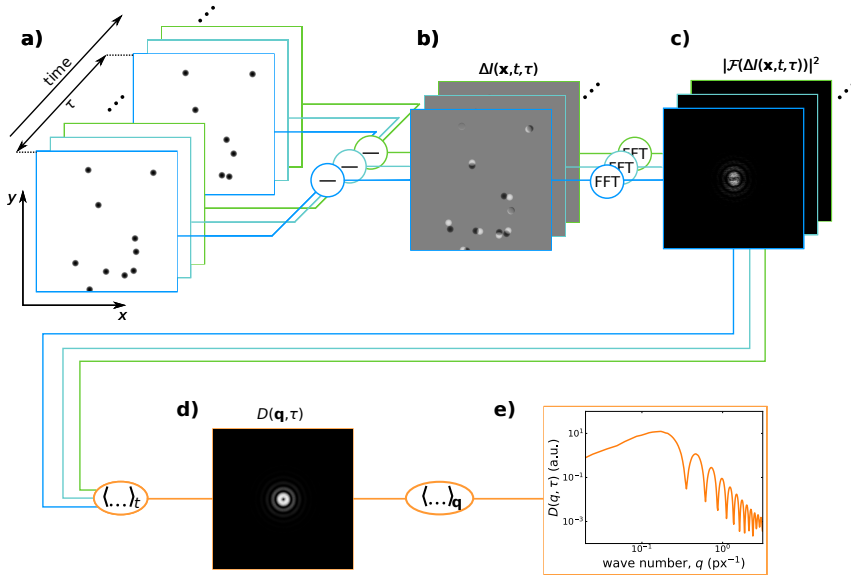
The image structure function $D(\mathbf{q}, \tau)$



The image structure function $D(\mathbf{q}, \tau)$

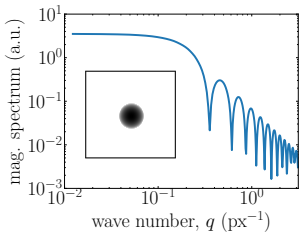
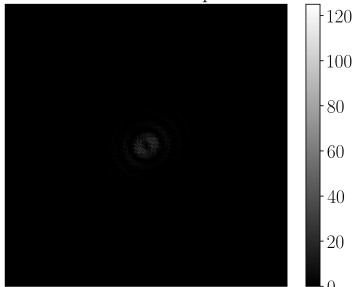


The image structure function $D(\mathbf{q}, \tau)$



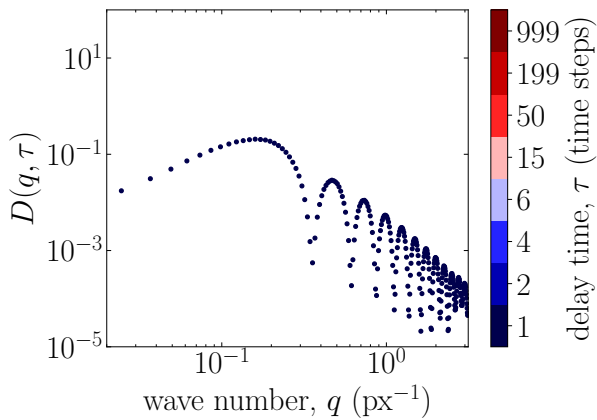
The image structure function $D(q, \tau)$

$\tau = 1$ time steps



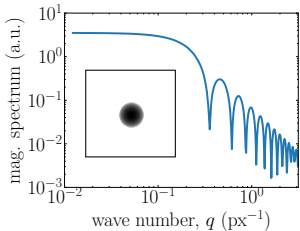
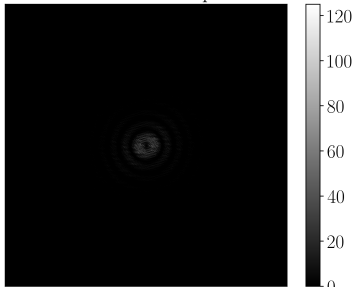
Time averaging: $D(\mathbf{q}, \tau) = \langle |\mathcal{F}(\Delta I)|^2 \rangle_t$

Azimuthal averaging: $D(\mathbf{q}, \tau) \rightarrow D(\mathbf{q}, \tau) \dots$



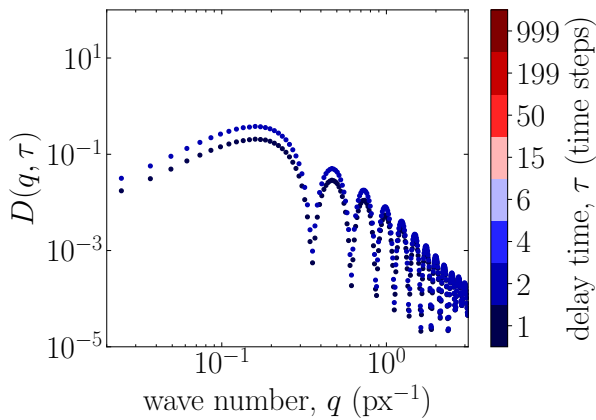
The image structure function $D(q, \tau)$

$\tau = 2$ time steps



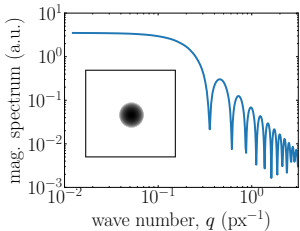
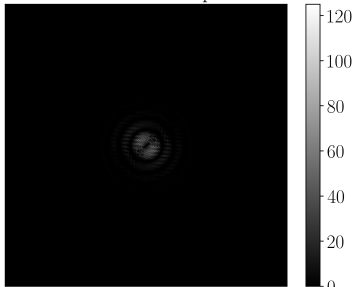
Time averaging: $D(\mathbf{q}, \tau) = \langle |\mathcal{F}(\Delta I)|^2 \rangle_t$

Azimuthal averaging: $D(\mathbf{q}, \tau) \rightarrow D(\mathbf{q}, \tau) \dots$



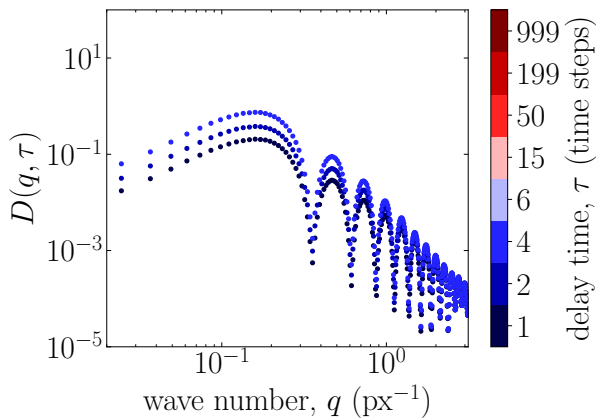
The image structure function $D(q, \tau)$

$\tau = 4$ time steps



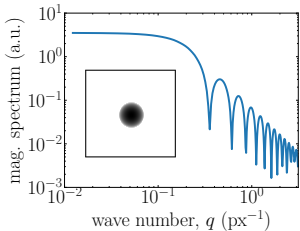
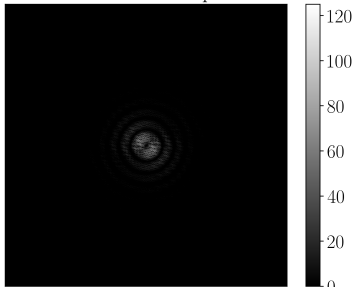
Time averaging: $D(\mathbf{q}, \tau) = \langle |\mathcal{F}(\Delta I)|^2 \rangle_t$

Azimuthal averaging: $D(\mathbf{q}, \tau) \rightarrow D(\mathbf{q}, \tau) \dots$



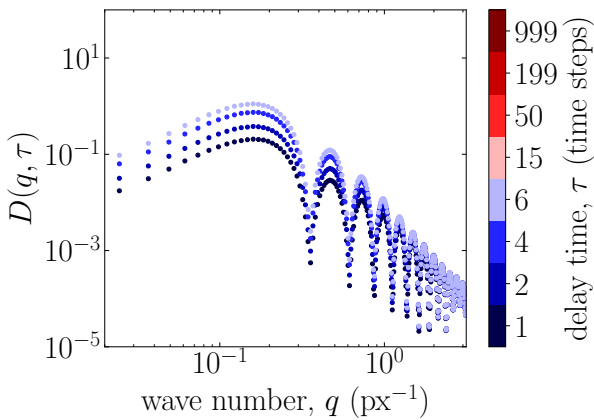
The image structure function $D(q, \tau)$

$\tau = 6$ time steps

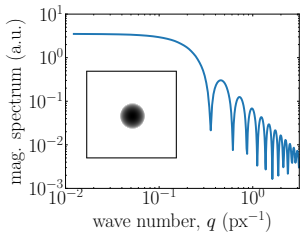
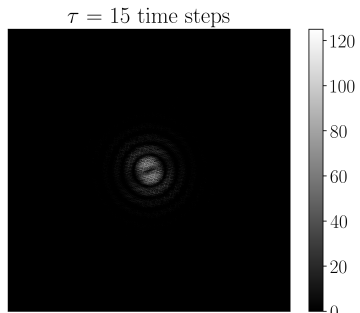


Time averaging: $D(\mathbf{q}, \tau) = \langle |\mathcal{F}(\Delta I)|^2 \rangle_t$

Azimuthal averaging: $D(\mathbf{q}, \tau) \rightarrow D(\mathbf{q}, \tau) \dots$

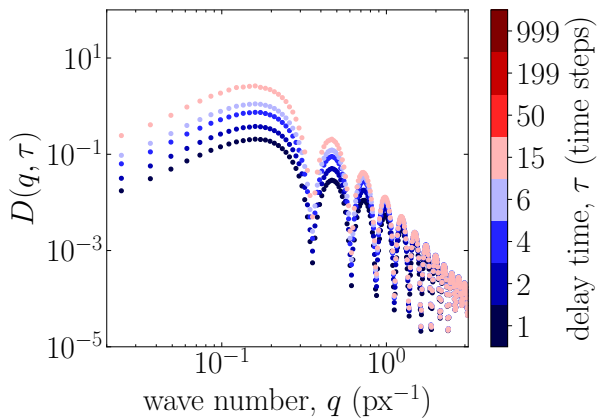


The image structure function $D(q, \tau)$

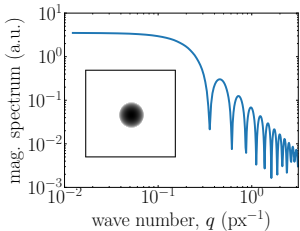
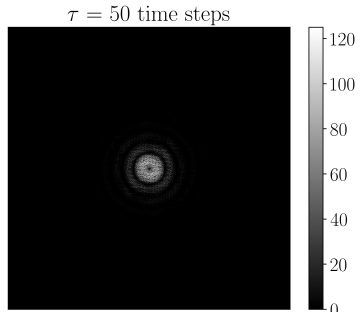


Time averaging: $D(\mathbf{q}, \tau) = \langle |\mathcal{F}(\Delta I)|^2 \rangle_t$

Azimuthal averaging: $D(\mathbf{q}, \tau) \rightarrow D(\mathbf{q}, \tau) \dots$

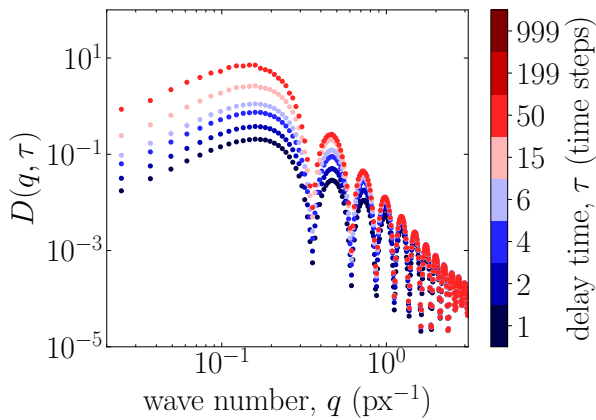


The image structure function $D(q, \tau)$

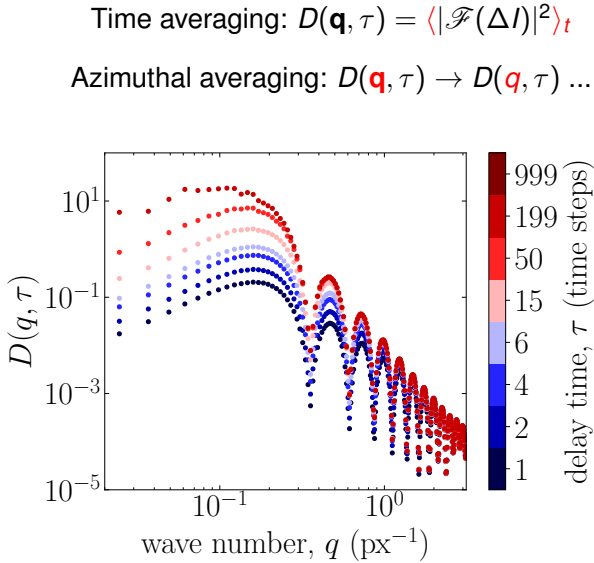
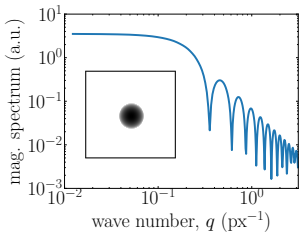
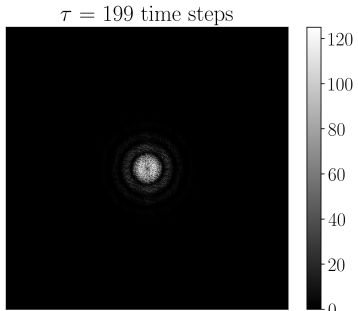


Time averaging: $D(\mathbf{q}, \tau) = \langle |\mathcal{F}(\Delta I)|^2 \rangle_t$

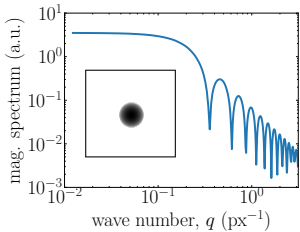
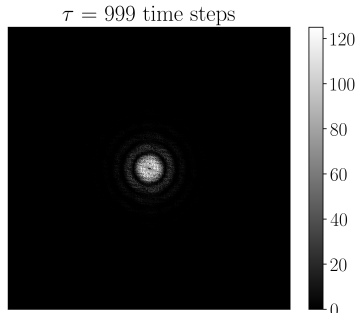
Azimuthal averaging: $D(\mathbf{q}, \tau) \rightarrow D(\mathbf{q}, \tau) \dots$



The image structure function $D(q, \tau)$

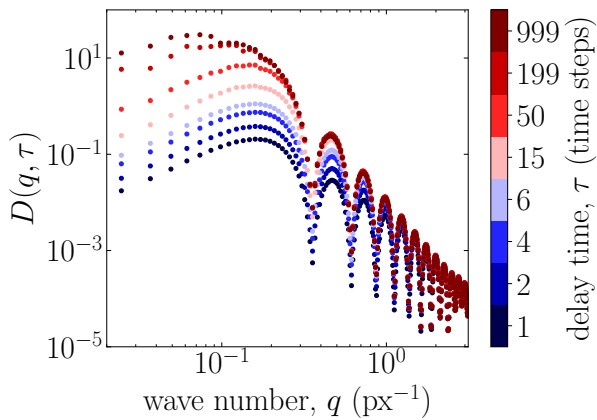


The image structure function $D(q, \tau)$

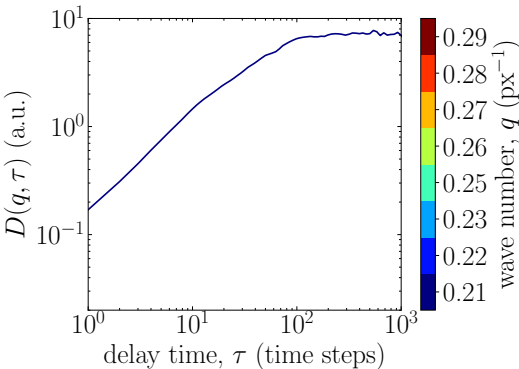
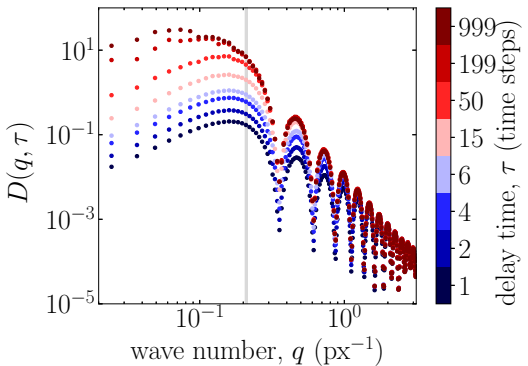


Time averaging: $D(\mathbf{q}, \tau) = \langle |\mathcal{F}(\Delta I)|^2 \rangle_t$

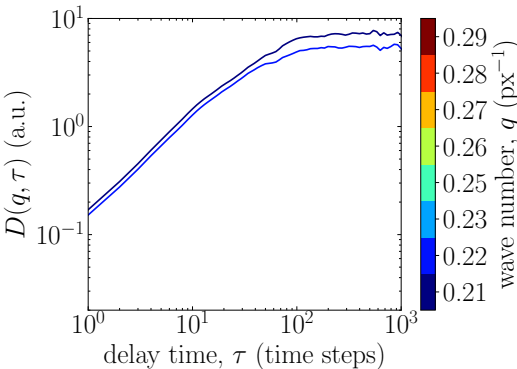
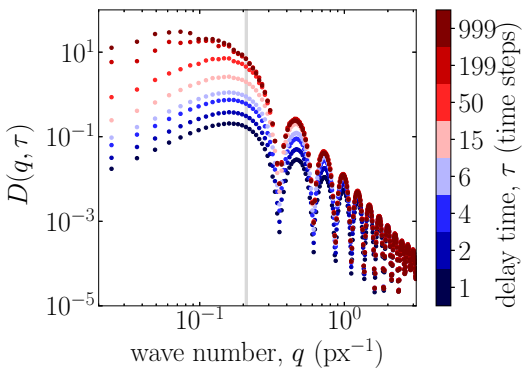
Azimuthal averaging: $D(\mathbf{q}, \tau) \rightarrow D(\mathbf{q}, \tau) \dots$



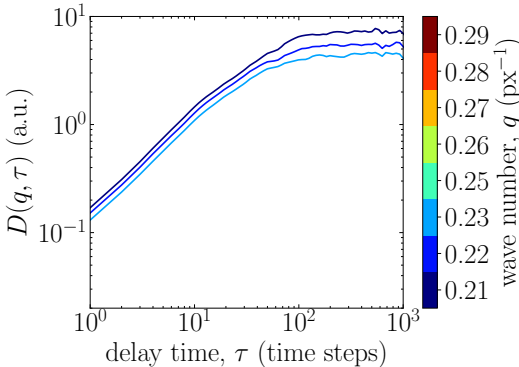
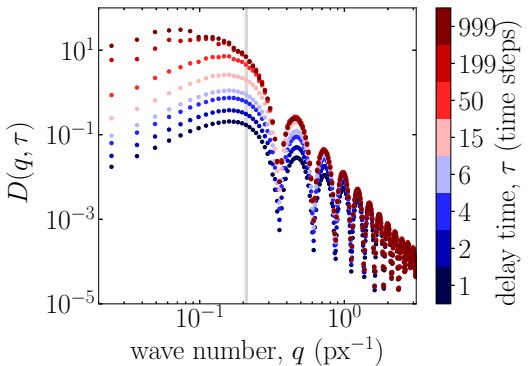
The image structure function $D(q, \tau)$



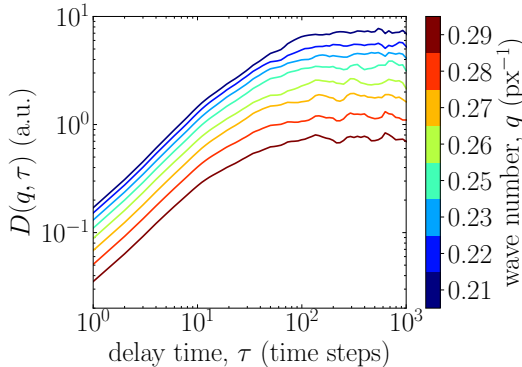
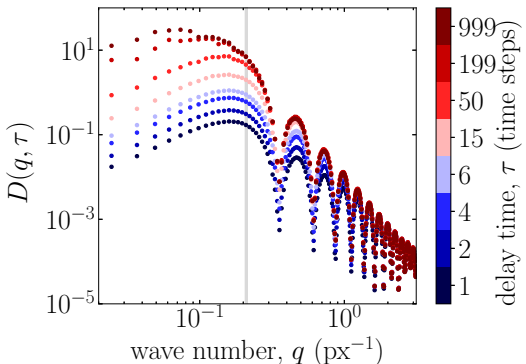
The image structure function $D(q, \tau)$



The image structure function $D(q, \tau)$

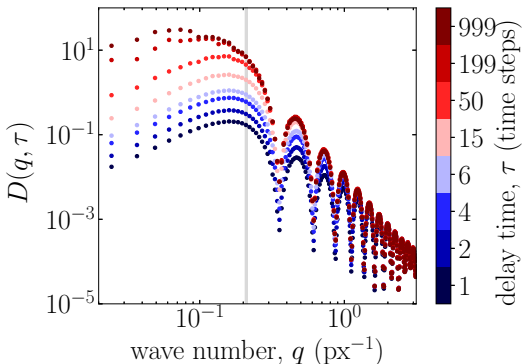


The image structure function $D(q, \tau)$

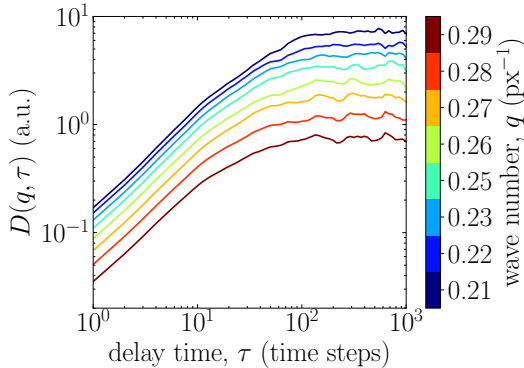


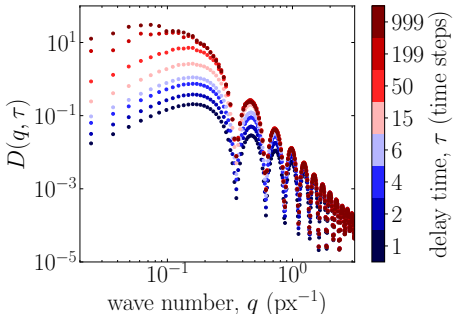
$$\begin{aligned} D(q, \tau) &= \left\langle |I(q, t + \tau) - I(q, t)|^2 \right\rangle_t \\ &= A(q) \left[1 - \frac{\left\langle I^*(q, t) I(q, t + \tau) \right\rangle_t}{\left\langle |I(q, t)|^2 \right\rangle_t} \right] + B(q) \end{aligned}$$

The image structure function $D(q, \tau)$

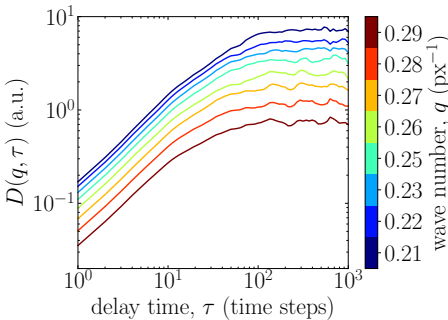


$$\begin{aligned}
 D(q, \tau) &= \left\langle |I(q, t + \tau) - I(q, t)|^2 \right\rangle_t \\
 &= A(q) \underbrace{\left[1 - \frac{\left\langle I^*(q, t) I(q, t + \tau) \right\rangle_t}{\left\langle |I(q, t)|^2 \right\rangle_t} \right]}_{\text{Image correlation function}} + B(q)
 \end{aligned}$$





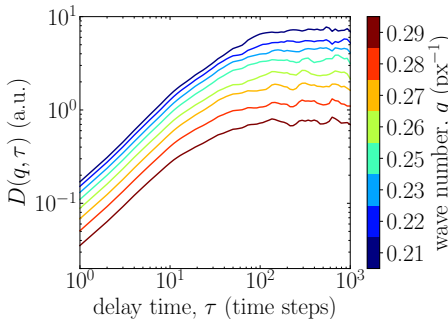
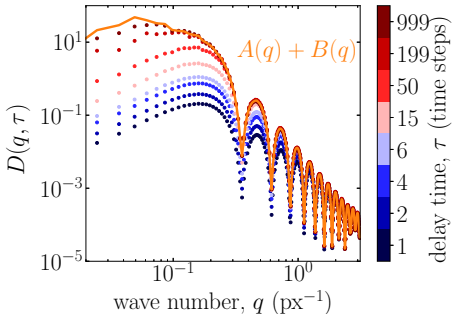
$$\begin{aligned}
 D(q, \tau) &= \left\langle |I(q, t + \tau) - I(q, t)|^2 \right\rangle_t \\
 &= A(q) \underbrace{\left[1 - \frac{\langle I^*(q, t) I(q, t + \tau) \rangle_t}{\langle |I(q, t)|^2 \rangle_t} \right]}_{\text{Image correlation function}} + B(q)
 \end{aligned}$$



Linear space invariant imaging

$$f(q, \tau) = \frac{\langle \rho^*(q, t) \rho(q, t + \tau) \rangle_t}{\langle |\rho(q, t)|^2 \rangle_t}$$

Intermediate scattering function



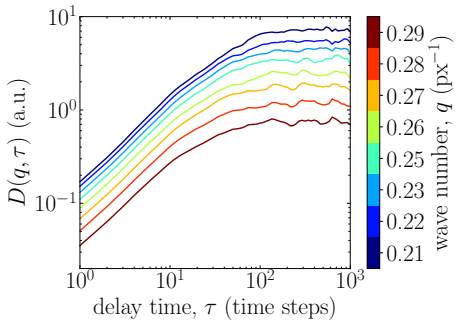
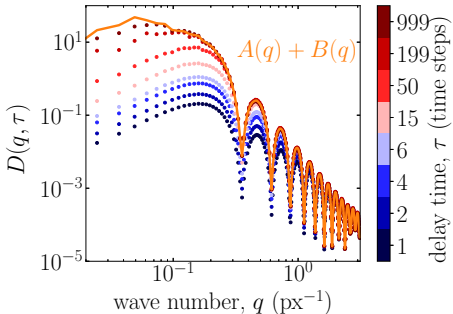
$$\begin{aligned}
 D(q, \tau) &= \left\langle |I(q, t + \tau) - I(q, t)|^2 \right\rangle_t \\
 &= \textcolor{orange}{A}(q) \left[1 - \frac{\langle I^*(q, t) I(q, t + \tau) \rangle_t}{\langle |I(q, t)|^2 \rangle_t} \right] + \textcolor{green}{B}(q)
 \end{aligned}$$

- $D(q, \tau \rightarrow 0) = \textcolor{green}{B}(q) = 0$
- $D(q, \tau \rightarrow \infty) = \textcolor{orange}{A}(q) + \textcolor{orange}{B}(q)$

Linear space invariant imaging

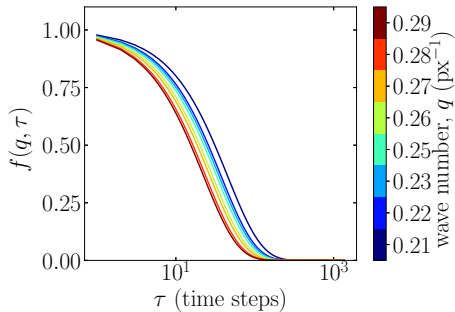
$$f(q, \tau) = \frac{\langle \rho^*(q, t) \rho(q, t + \tau) \rangle_t}{\langle |\rho(q, t)|^2 \rangle_t}$$

Intermediate scattering function



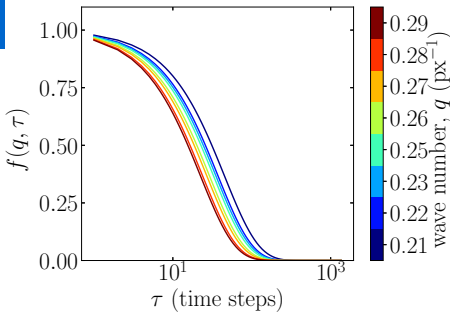
$$\begin{aligned} D(q, \tau) &= \left\langle |I(q, t + \tau) - I(q, t)|^2 \right\rangle_t \\ &= A(q) \left[1 - \frac{\langle I^*(q, t) I(q, t + \tau) \rangle_t}{\langle |I(q, t)|^2 \rangle_t} \right] + B(q) \end{aligned}$$

- $D(q, \tau \rightarrow 0) = B(q) = 0$
- $D(q, \tau \rightarrow \infty) = A(q) + B(q)$



Intermediate scattering function $f(q, \tau)$

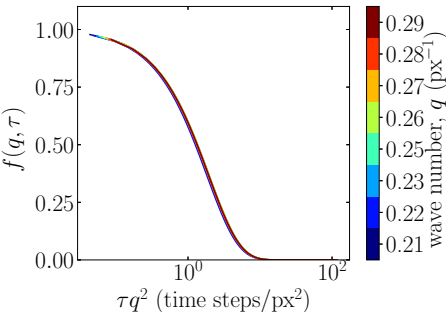
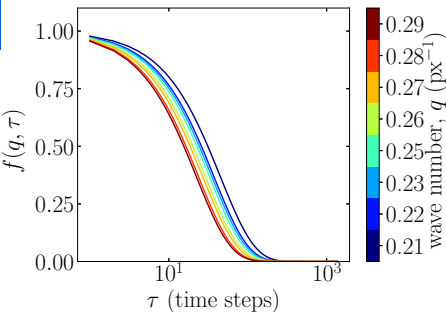
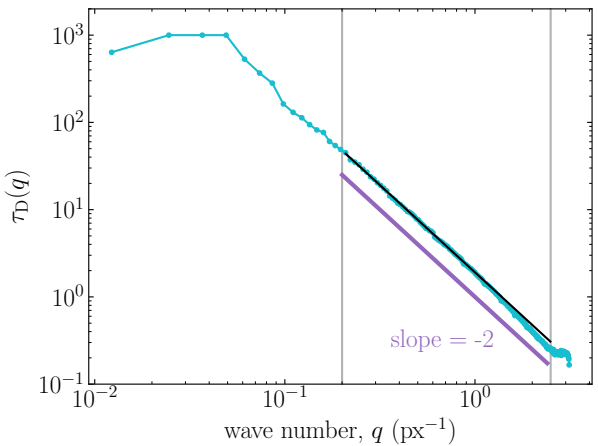
Brownian motion:
 $f(q, \tau) = \exp(-q^2 \tau / \tau_D)$



Intermediate scattering function $f(q, \tau)$

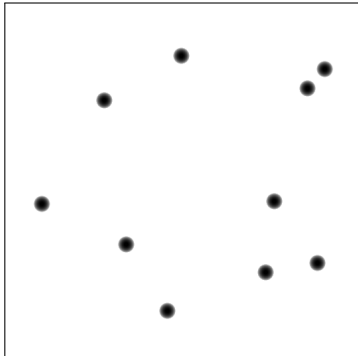
Brownian motion:

$$f(q, \tau) = \exp(-q^2 \tau / \tau_D)$$

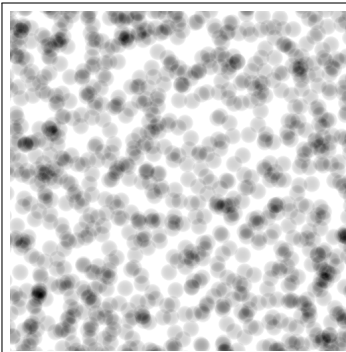


Accuracy of X-DFA: Varying the number of particles

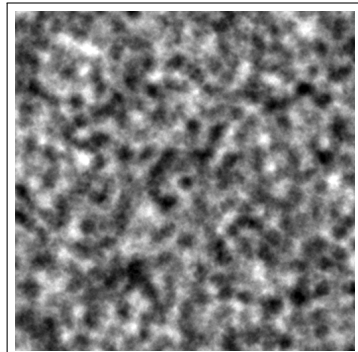
10 particles



1000 particles



100 000 particles



Deviation from the simulation input:

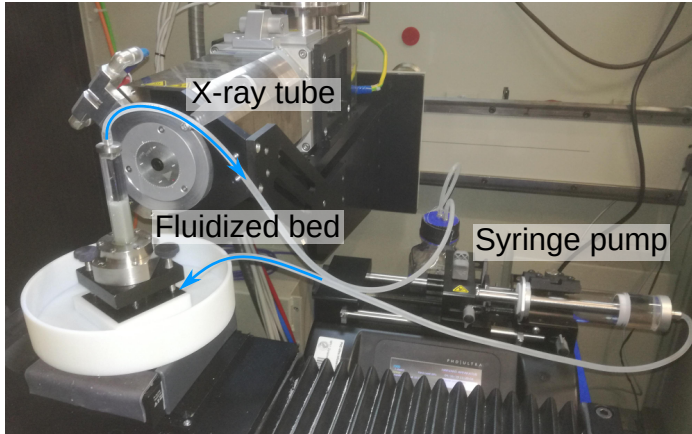
6%

2%

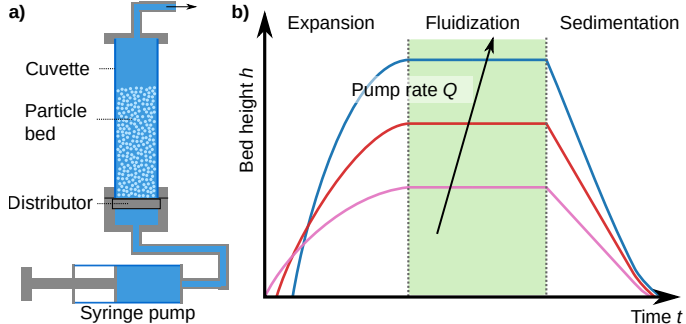
2%

PIV off by $\approx 650\%$

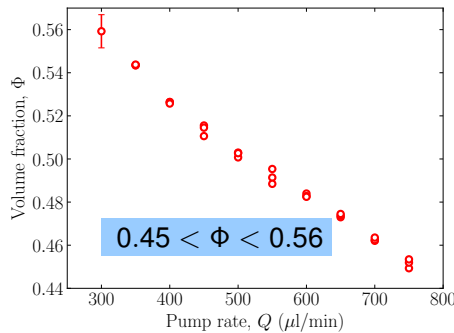
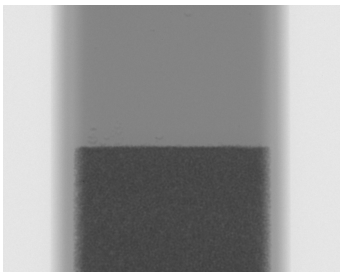
Experimental validation of X-DFA: A suspension of sedimenting particles



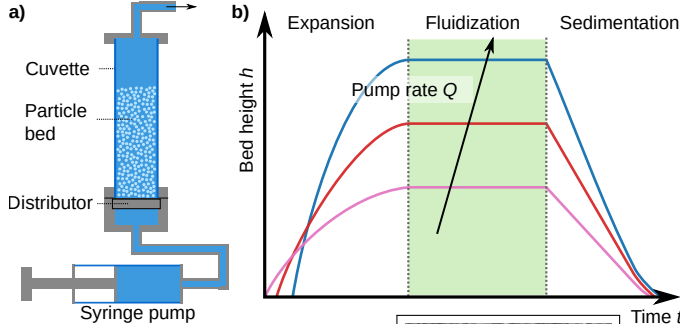
Experimental validation of X-DFA: A suspension of sedimenting particles



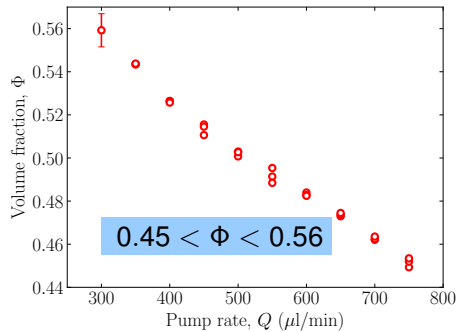
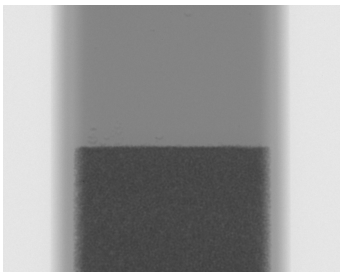
X-ray radiography



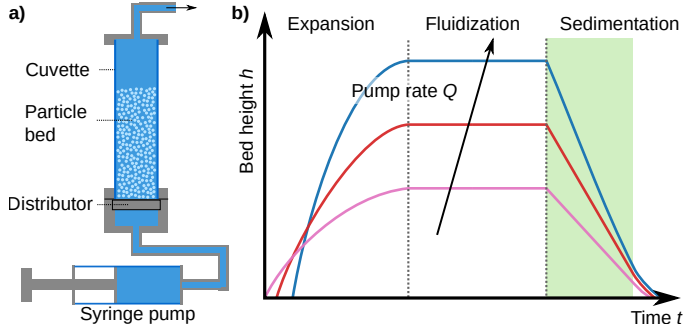
Experimental validation of X-DFA: A suspension of sedimenting particles



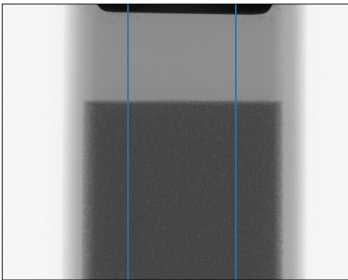
X-ray radiography



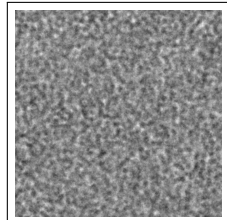
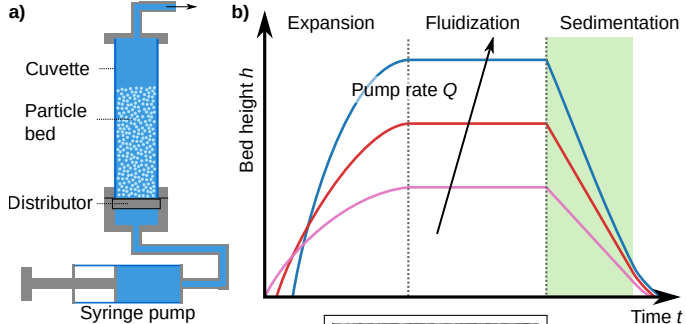
Experimental validation of X-DFA: A suspension of sedimenting particles



X-ray radiography

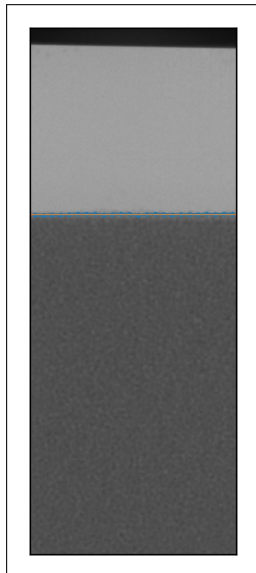


Experimental validation of X-DFA: A suspension of sedimenting particles

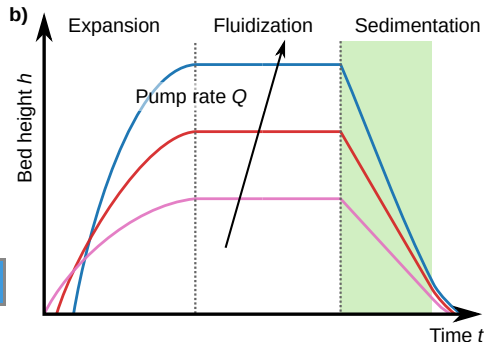
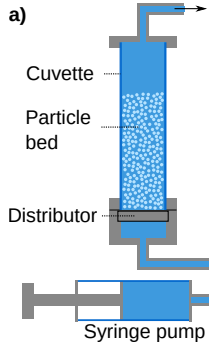


Comparison of
 $\langle v \rangle_{\text{dfa}}$ and $\langle v \rangle_{\text{front}}$

X-ray radiography

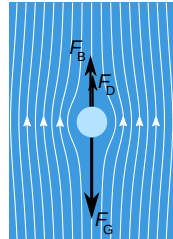


Liquid fluidized bed: Richardson-Zaki law



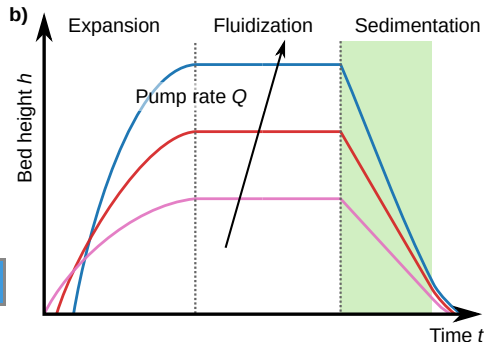
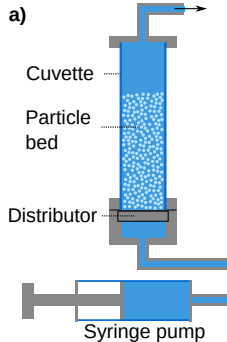
Gravitation Buoyancy Drag

$$F_G = F_B + F_D$$



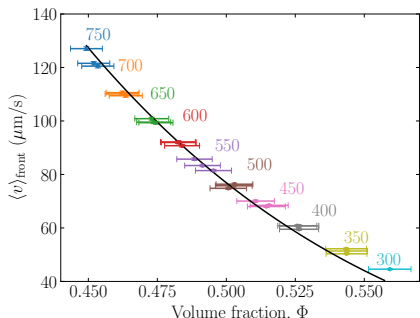
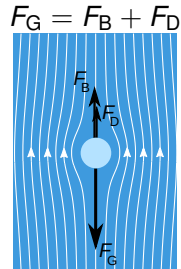
$$\frac{\langle v \rangle_{\text{fluid}}}{v_{\text{Stokes}}} = (1 - \Phi)^n$$

Liquid fluidized bed: Richardson-Zaki law

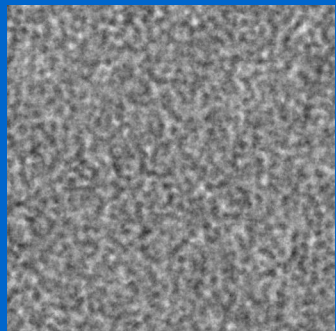
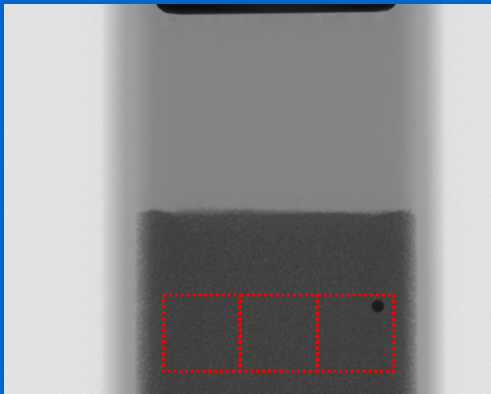


$$\frac{\langle v \rangle_{\text{front}}}{v_{\text{Stokes}}} = (1 - \Phi)^n$$

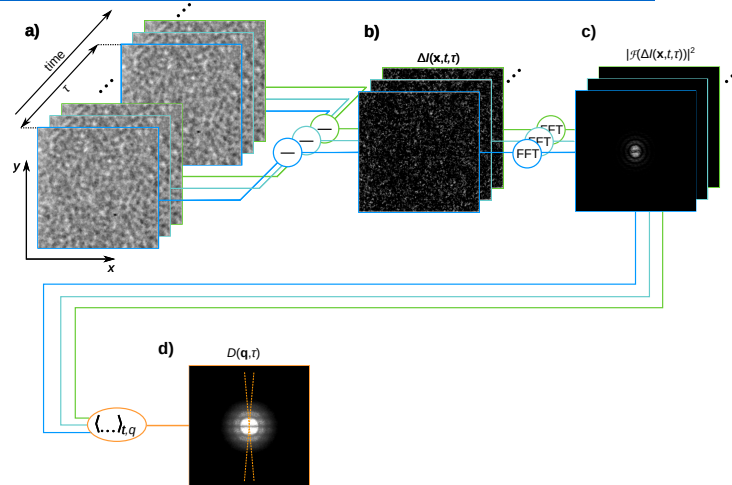
Gravitation Buoyancy Drag



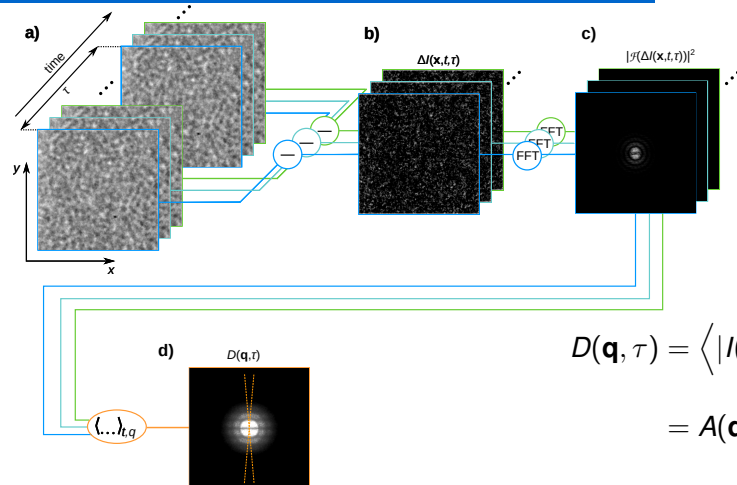
X-ray Digital Fourier Analysis of a suspension of sedimenting particles



The image structure function $D(\mathbf{q}, \tau)$



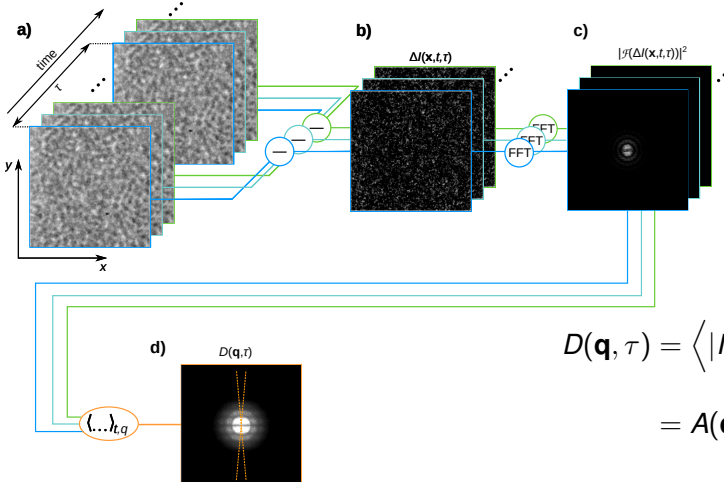
The image structure function $D(\mathbf{q}, \tau)$



$$\begin{aligned} D(\mathbf{q}, \tau) &= \left\langle |I(\mathbf{q}, t + \tau) - I(\mathbf{q}, t)|^2 \right\rangle_t \\ &= A(\mathbf{q}) \left[1 - \frac{\langle I^*(\mathbf{q}, t) I(\mathbf{q}, t + \tau) \rangle_t}{\langle |I(\mathbf{q}, t)|^2 \rangle_t} \right] + B(\mathbf{q}) \end{aligned}$$

- $D(\mathbf{q}, \tau \rightarrow 0) = B(\mathbf{q})$
- $D(\mathbf{q}, \tau \rightarrow \infty) = A(\mathbf{q}) + B(\mathbf{q})$

The image structure function $D(\mathbf{q}, \tau)$



Linear space invariant imaging

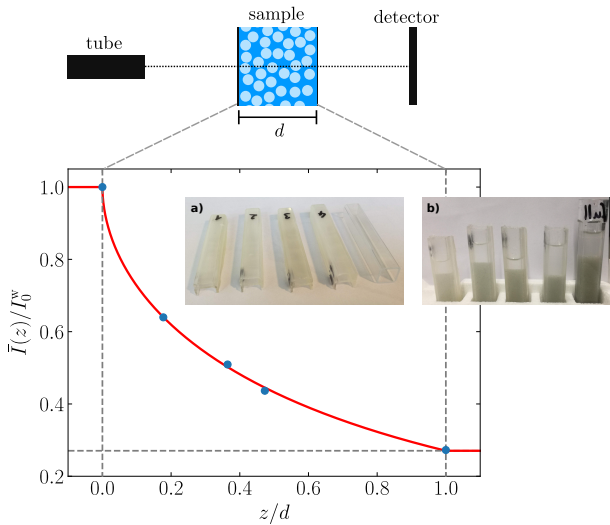
$$f(\mathbf{q}, \tau) = \frac{\langle \rho^*(\mathbf{q}, t)\rho(\mathbf{q}, t + \tau) \rangle_t}{\langle |\rho(\mathbf{q}, t)|^2 \rangle_t}$$

Intermediate scattering function

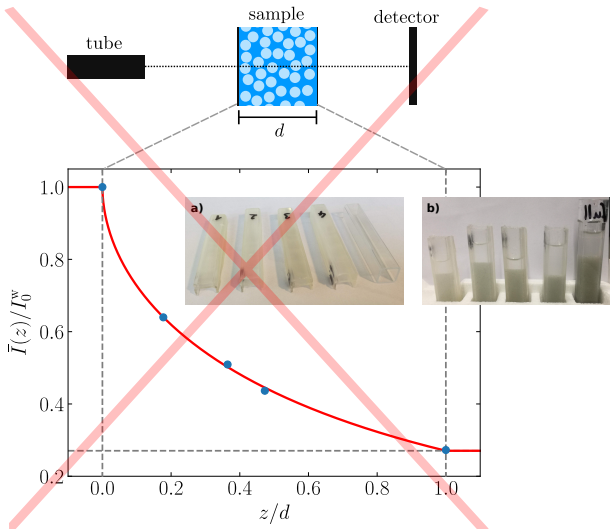
$$\begin{aligned} D(\mathbf{q}, \tau) &= \left\langle |I(\mathbf{q}, t + \tau) - I(\mathbf{q}, t)|^2 \right\rangle_t \\ &= A(\mathbf{q}) \left[1 - \frac{\langle I^*(\mathbf{q}, t)I(\mathbf{q}, t + \tau) \rangle_t}{\langle |I(\mathbf{q}, t)|^2 \rangle_t} \right] + B(\mathbf{q}) \end{aligned}$$

- $D(\mathbf{q}, \tau \rightarrow 0) = B(\mathbf{q})$
- $D(\mathbf{q}, \tau \rightarrow \infty) = A(\mathbf{q}) + B(\mathbf{q})$

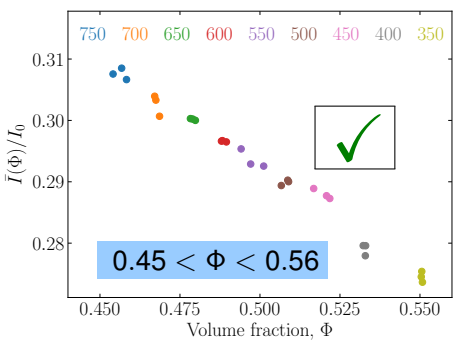
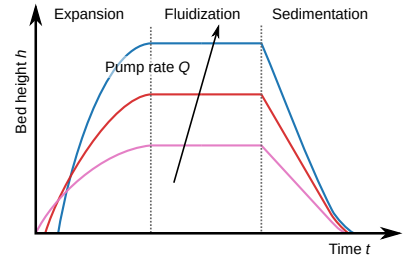
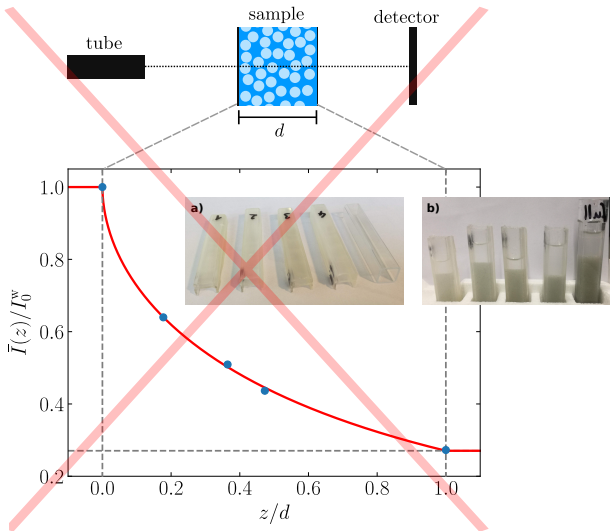
X-ray imaging – Linear space invariant?



X-ray imaging – Linear space invariant?



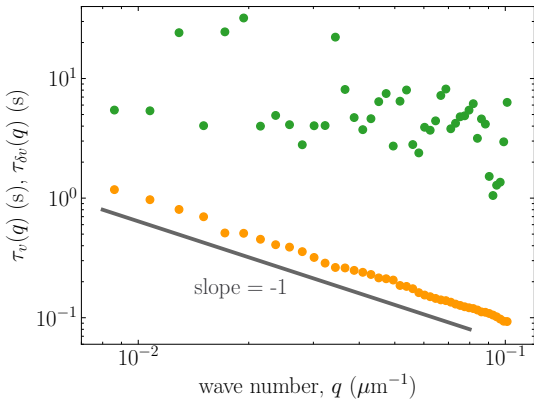
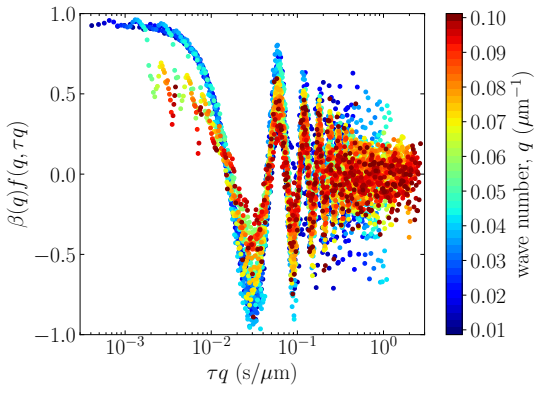
X-ray imaging – Linear space invariant?



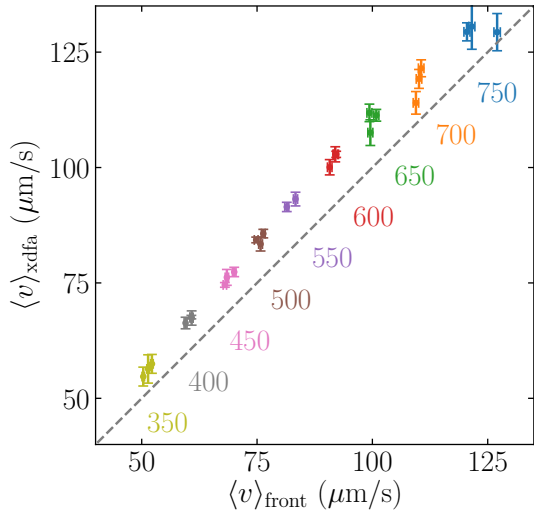
X-DFA for a suspension of sedimenting particles

$$f(q, \tau) = \cos(q\langle v_s \rangle \tau) \exp\left(-\frac{1}{2}q^2 \delta v^2 \tau^2\right)$$

$$\langle v_s \rangle = \langle \Delta r \rangle / \tau_\nu, \langle \delta v \rangle = \langle \delta r \rangle / \tau_{\delta\nu}$$

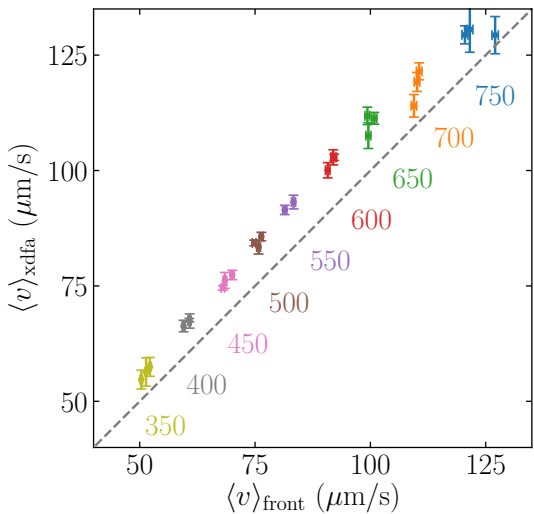


Front tracking vs. X-DFA

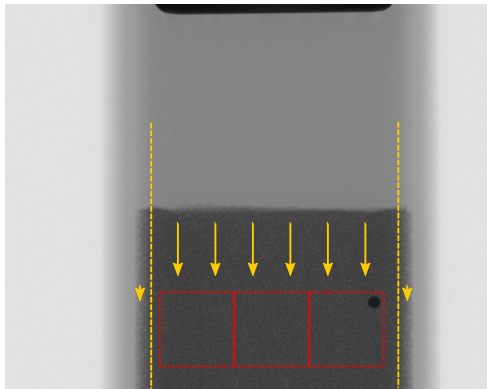


$\langle v \rangle_{\text{xdfa}} > \langle v \rangle_{\text{front}}$ by 9.4%

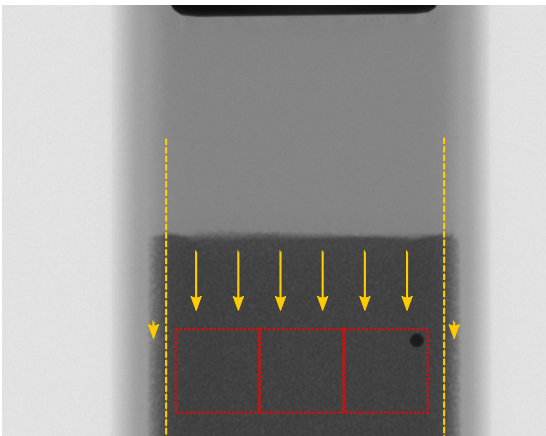
Front tracking vs. X-DFA



$\langle v \rangle_{\text{xdfa}} > \langle v \rangle_{\text{front}}$ by 9.4%

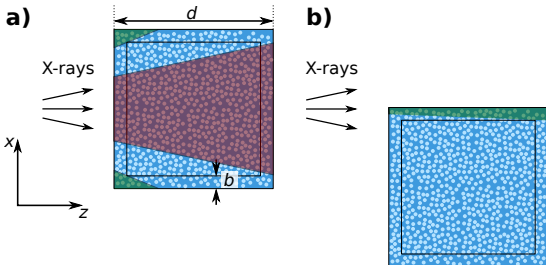


Estimate width of boundary layer



$\langle v \rangle_{\text{xdfa}} > \langle v \rangle_{\text{front}}$ by 9.4%

$\langle v \rangle_{\text{xdfa}}$ takes two layers into account
 $\langle v \rangle_{\text{front}}$ takes four layers into account



Estimation:

Boundary velocity = 0

Else = const.

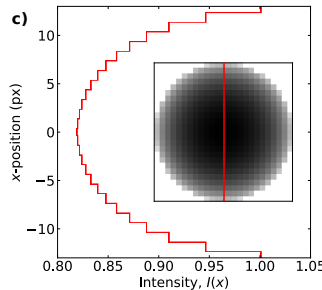
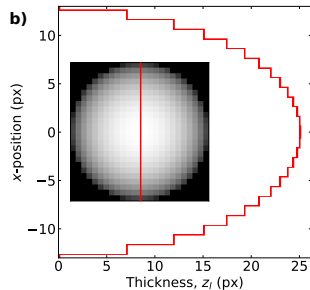
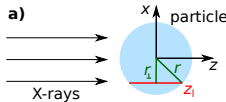
→ $b \approx 3$ particle diameters

Thank you for your attention!



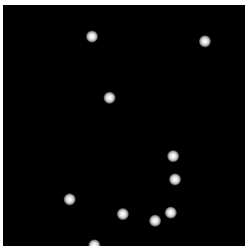
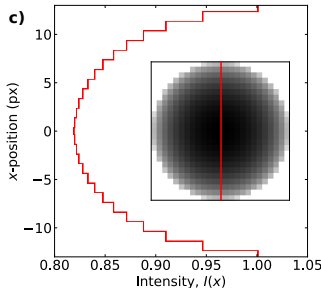
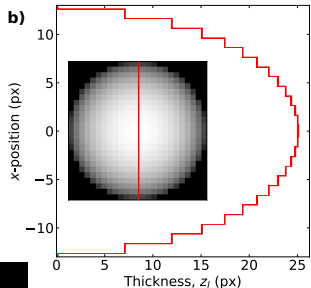
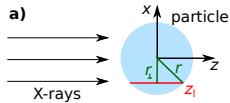
Backup slides

Synthetic radiograms

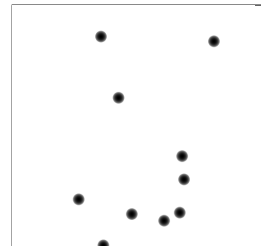


Beer-Lambert
 $I(z_l) = I_0 \exp(-\mu z)$

Synthetic radiograms



Beer-Lambert
 $I(z_l) = I_0 \exp(-\mu z)$



Linear space invariant imaging

Image correlation function

$$g(\mathbf{q}, \tau) = \frac{\langle I^*(\mathbf{q}, t)I(\mathbf{q}, t + \tau) \rangle_t}{\langle |I(\mathbf{q}, t)|^2 \rangle_t}$$

Linear space invariant imaging

Image correlation function

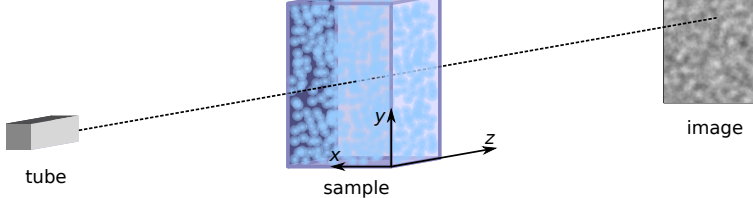
$$g(\mathbf{q}, \tau) = \frac{\langle I^*(\mathbf{q}, t)I(\mathbf{q}, t + \tau) \rangle_t}{\langle |I(\mathbf{q}, t)|^2 \rangle_t}$$

Intermediate scattering function

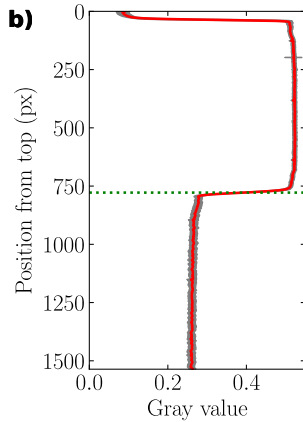
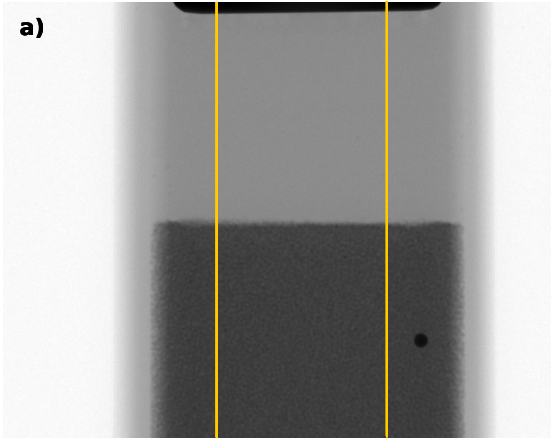
$$f(\mathbf{q}, \tau) = \frac{\langle \rho^*(\mathbf{q}, t)\rho(\mathbf{q}, t + \tau) \rangle_t}{\langle |\rho(\mathbf{q}, t)|^2 \rangle_t}$$

Linear space-invariant imaging:

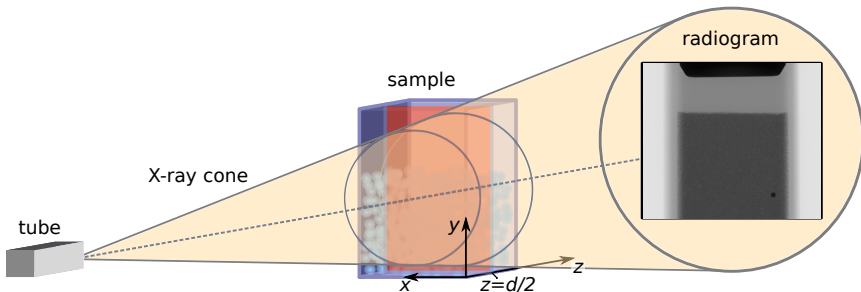
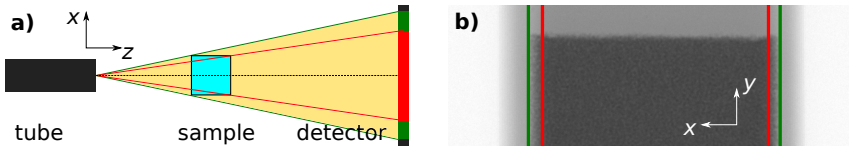
$$I(\mathbf{r}, t) = I_0 + \int d\mathbf{r}' dz' T(\mathbf{r} - \mathbf{r}', -z') c(\mathbf{r}', z', t)$$



Tracking of particle front



Tracking of particle front



Tracking of particle front

